Glass fabric reinforced cementitious matrix: Tensile properties and bond performance on masonry substrate

Marianovella Leone [a, *], Maria Antonietta Aiello [a], Alberto Balsamo [b], Francesca Giulia Carozzi [c], Francesca Ceroni [d], Marco Corradi [e, f], Matija Gams [g], Enrico Garbin [h], Natalino Gattesco [i], Piotr Krajewski [j], Claudio Mazzotti [k], Daniel Oliveira [l], Catherine Papanicolaou [m], Giovanna Ranocchiai [n], Francesca Roscini [o], Dorothea Saenger [p]

[a] Department of Engineering for Innovation, University of Salento, Lecce, Italy
[b] Department of Structures for Engineering and Architecture, University of Naples "Federico II", Via Claudio 21, 80125 Naples, Italy
[c] Department of Architecture, Built Environment and Construction Engineering, Politecnico di Milano, Milan, Italy
[d] Engineering Department, University of Napoli 'Parthenope', Centro Direzionale is. C4, 80143 Napoli, Italy
[e] Northumbria University, Mechanical and Construction Engineering Department, Wynne-Jones Building, NE1 8ST, Newcastle Upon Tyne, United Kingdom
[f] University of Perugia, Department of Engineering, Via Duranti, 93, 06125 Perugia, Italy
[g] ZAG, Slovenian National Building and Civil Engineering Institute, Department of Structures, Dimičeva Ulica 12, 1000 Ljubljana, Slovenia
[h] Department of Civil, Environmental and Architectural Engineering, University of Padova, Padua, Italy
[i] Department of Engineering and Architecture, University of Trieste, Piazzale Europa 1, 34127 Trieste, Italy
[j] Faculty of Civil Engineering, Cracow University of Technology, Warszawska 24, 31-155 Cracow, Poland
[k] Department of Civil, Chemical, Environmental, and Materials Engineering, Alma Mater Studiorum University of Bologna, Bologna, Italy
[l] Department of Civil Engineering, University of Minho, Campus de Azurém, 4800-058 Guimarães, Portugal
[m] Department of Civil Engineering, University of Patras, 26500 Patras, Greece
[n] Department of Civil and Environmental Engineering, University of Florence, 50139 Florence, Italy
[o] Department of Engineering, Roma Tre University, Rome, Italy
[p] Institute of Building Materials Research, Chair of Building Materials, RWTH Aachen University, Schinkelstrasse 3, 52062 Aachen, Germany

ARTICLE INFO

ABSTRACT

Fibre-reinforced composite materials have gained an increasing success, mostly for strengthening, retrofitting, and repairing existing structures. However some problems may arise with the use of traditional FRP (Fiber Reinforced Polymer), particularly when the compatibility with the substrate and the reversibility of the intervention are required, as in case of cultural heritage buildings, or specific exposition conditions may compromise the long term effectiveness of the reinforcement, as in presence of high temperature and humidity. Starting from these considerations new composite materials are emerging as a more effective solution in certain fields of application and under specific service conditions; in this context, mortar-based composite systems, consisting of one or more layers of uni- or bi-directional fibre nets embedded in cement/lime-based matrix layers, can be used as reinforcement of both concrete and masonry structures. However, the research work dealing with these emerging materials and their performances when used as a strengthening system for existing structures is still limited. Both experimental and theoretical investigations are needed in order to deliver reliable design methodologies. In this work, a Round Robin Test aimed to the characterization of both bond with the existing substrate and tensile performance of glass fabric (in the form of grids) coupled with inorganic mortar matrices is presented. The investigation was conducted at fifteen laboratories involved in the RILEM Technical Committee 250-CSM (Composites for the Sustainable Strengthening of Masonry). With the aim of studying the bond behaviour between Fabric Reinforced Cementitious Matrix (FRCM) composites and masonry substrate, single and double lap shear tests were carried out on brick-masonry prisms. Results provide useful informations about the mechanical properties, the bond capacity and the failure mechanisms of different commercially available glass FRCM systems. Finally, critical aspects are underlined to address the progress of the research work.

© 2017 Elsevier Ltd. All rights reserved.

---

1. Introduction

The assessment of new retrofitting techniques is an important issue while enabling the design optimization when the safety of existing structures is addressed. Composite materials, among all Glass Fibre Reinforced Polymers (GFRP), have been used in structural applications since the first half of 20th century, however the high cost and the unfamiliarity with their mechanical behaviour (i.e. anisotropy) had slowed down their wide spread use in civil engineering.

In recent years, the use of GFRP materials (bars, plates, sheets) as external reinforcement for concrete structures has grown due to their superior properties compared to steel in terms of corrosion and fatigue resistance, lightweight characteristics, and high tensile strength to weight ratio. While an extensive research has been conducted for reinforced concrete structures strengthened by composite materials, limited work is still available when masonry constructions are concerned. The use of GFRPs to strengthen masonry structures first appeared in the USA in the 90s, where GFRPs strips epoxy bonded to the masonry substrate were utilized. However, the cost of GFRP (referring to both the composite material and the epoxy adhesive) and a mechanical improvement of the structure comparable to that obtained by conventional retrofitting methods has limited a widespread use of GFRPs as external reinforcement of masonry structures.

On the other hand, catastrophic earthquakes in many areas of the world have revealed the high vulnerability of masonry buildings, traditionally designed without special measures against the effects of horizontal loads. The damages caused by seismic actions on masonry buildings involved loss of human life, high costs of repairing and, in many cases, irreversible loss of cultural heritage.

Historic buildings represent a peculiar class of constructions not only because of their architectural value but also because of their social role. The need to be repaired or retrofitted is increased in the last years and this task is particularly challenging in earthquake-prone areas. Between 1995 and 2015, a series of experiments were carried out at several research centers across Europe and USA to assess effective strengthening techniques for historic masonry using GFRP materials (in the form of overlays, wraps or pre-preg laminates). The principal focus has been the structural upgrade of masonry elements against in-plane seismic action using continuous glass fibres sheet and GFRP plates, usually made by unidirectional fibres [1–9] Vaults and arches also received considerable attention in many papers dealing with GFRP reinforcements applied at the intrados or extrados of the curved elements [10–17]. Other papers have considered the reinforcement of stone or brick masonry columns by providing a confinement action using glass fibres [18–25]. In the last few years, many researchers have also investigated the bond between FRPs and masonry substrates by means of single and double face shear tests [26–40]. Thanks to the wide research efforts national and international guidelines have been assessed and now available for the design of unreinforced masonry structures strengthened by Externally Bonded EB-FRP systems [41,42].

A more innovative technique has been recently proposed in several studies [43–62]. In the early 2010s, the use of inorganic matrices/adhesives was considered with the aim to improve the long term behaviour of the strengthening intervention and meet the requirements of conservation of historic masonry structures, including reinforcement reversibility and reinforcement-to-substrate compatibility. This type of matrix, generally including cementitious and lime-based materials, has limited concerns regarding the cost, the health and the safety restrictions compared to organic adhesives. In this case, fibre rovings can be used in a dry or coated or resin-impregnated form.

According to the international [34] and Italian terminology the common acronym used to refer to these materials is FRCM (Fabric Reinforced Cementitious Matrix) which also account for system with cement-free matrices. Other acronyms as FRM (Fibre Reinforced Mortar) or TRM (Textile Reinforced Mortar) are often utilized.

The use of inorganic matrices needs to be validated with extensive research activities; their mechanical properties are significantly weaker compared to those of epoxy adhesives. In particular in the case of dry fibre grids the type of matrix and its thickness may greatly influences the mechanical performance of the composites.

In addition, the composite action of materials made by inorganic matrices and high performance fibers should be studied in depth. In the case of FRCM it is necessary to use alternative forms of fabric layouts: a 2D grid-like configuration constituted by fibre rovings arranged in (typically) two orthogonal directions provides the necessary mechanical interlock between the reinforcement (the grid or the textile) and the binding (the mortar that protrudes through the grid's openings) ensuring an adequate composite action. In addition, in the case of dry fibre rovings, the matrix-to-reinforcement bond characteristics are further enhanced by the eventual penetration of the mortar paste into the bundles.

In this paper, the analysis of the mechanical properties of Fibre Reinforced Cementitious Mortar specimens in terms of tensile and bond capacity are investigated. Due to the growing interest in the area of composite materials made by an inorganic matrix and the extremely high combination of variables associated with the use of FRCM, a wide research activity is needed. The aim of the present work is to contribute in deepening the knowledge on this topic enriching the limited existing literature. To this scope, fifteen laboratories have tested eight commercially available products that employ lime- or cement-based matrices. Research labs involved include: Cracow University of Technology (Cut), RWTH Aachen University (Aachen), Slovenian National Building and Civil Engineering Institute (ZAG), Polytechnic di Milano (Polimi), University of Bologna (Unibo), University of Firenze (Unifi), University of Minho (Uminho), University of Naples "Federico II" (Unina), University of Napoli 'Parthenope' (Unisannio), University of Padova (Unipd), University of Patras (Upatras), University of Perugia (Unipg), University of Roma Tre (Unirm3), University of Salento (Unisalento), University of Trieste (Units). The results herein reported furnish interesting scientific founds concerning the mechanical performance of FRCM and highlight critical aspects to be further investigated.

The results discussed in the present work represent part of the activities of RILEM Technical Committee 250-CSM "Composites for Sustainable Strengthening of Masonry". In particular, the study of the tensile and bond performance of FRCM systems involving 21 research centers and laboratories and 11 companies was performed. The main objectives of the planned research work were the evaluation and the comparison of the mechanical properties of different FRCM materials, made by glass, carbon [63,64], basalt [65], aramid, PBO [66,67], and steel [68] textiles.

Based on the previous considerations, the composite response under direct tension, the critical assessment of the related failure modes as well as the identification of the substrate-to-composite and reinforcement-to-matrix bond mechanisms were analysed and discussed. The scope is to furnish an effective contribute to the understanding of the resisting mechanisms of masonry elements retrofitted by inorganic matrix and fibres mesh.

2. GFRCM materials

In this section, the main mechanical and geometrical properties of the materials tested are reported according to the data sheets supplied by the manufacturers. Table 1 and Table 2 show the mechanical and geometrical properties of the reinforcement and the mortar, respectively while in Fig. 1 the picture of the tested grids is reported. The equivalent thickness of Table 1 refers to a smeared fabric distribution.

Analysing Table 1, Table 2 and Fig. 1 it is possible to note the great difference between the analysed materials both from mechanical and geometrical point of view. In addition, it appears evident as the data furnished by the suppliers aren't homogeneous in some cases or lacks of specific information; thus indirect elaborations were made and reported when possible.

The nomenclature used for mortar consists of two indices: the first is always the letter "m" and the second is the name of the type of reinforcement, according to Table 3.

In the following the main geometrical and mechanical characteristic of the tested reinforcement are summarized according to the data sheet of the suppliers.

A: a balanced glass fibre grid with a 15 × 15 mm mesh size. The equivalent thickness is 0,04 mm and the Young's modulus is 72 GPa. The grid has been coupled with a hydraulic lime-based mortar (Type m-A) with a compressive strength ranging from 5 to 15 MPa. This wide range of compressive strength is linked to the curing time that, as well known, highly influences the mechanical performance.

#B: the grid is made by a pre-impregnated GFRP with different yarn spacing. The designations B-33, B-66 and B-99 have been used to identify the spacing equal to 33 × 33 mm, 66 × 66 mm and 99 × 99 mm, respectively. The GFRP strands consist of continuous Alkali-Resistant (AR) glass fibres impregnated with thermosetting epoxy-vinylester resin. Three mortars were also used to realize the FRCM specimens. m-B1 mortar is based on white-colour natural hydraulic lime, with a compressive strength of 8 MPa. A ready-to-use lime- and cement-based mortar (m-B2) has been utilized for the tests carried out at Unipg and Units. A similar mortar with higher content of cement (m-B3) has been used for the test campaign at Unisalento and Uminho. The manufacturer provides a compressive strength of 8 and 20 MPa for mortars m-B2 and m-B3, respectively.

#C: a bi-directional AR glass fibre grid with a high concentration of zirconium oxide (>19%). The grid is characterized by a square mesh (spacing 12 mm). The mortar coupled with the fiberglass is based on a natural hydraulic lime (m-C). The manufacturer indicates the presence of a bond enhancing agent inside the mortar.

#D: two different types of D grid have been used. Type D-1 is characterized by a 15 mm grid spacing and an equivalent thickness of 0,048 mm, while type D-2 has a smaller spacing (7,6 mm) and equivalent thickness (0,046 mm). Both grids are made with AR glass. The mortar used for specimens preparation is based on pozzolanic lime (m-D type).

#E: it is made by AR glass fibres. The fibres present a special surface treatment (treated with a coating), which improves the adhesion to the mortar. This grid has been coupled with mortar type m-E. The mortar is based on natural pozzolanic lime and siliceous aggregates; the compressive strength is greater than 15 MPa; this value was experimentally estimated also by the labs; at Upatras a value of 12,1 MPa was found while at Unipd the compressive strength of the mortar resulted equal to 16,5 MPa. The recorded difference is probably due the curing time, higher at Unipd than Unipatras.

#F: it is a grid made by AR glass and aramid rovings, (Fig. 1f). The grid is characterized by a mesh size and elongation at failure equal to 10 × 12,5 mm and 2%, respectively. The matrix is made of a natural lime-based mortar with a compressive strength greater than 15 MPa, as provided by the manufacturer. The Young's modulus of the mortar is 9 GPa.

#G: it is made by AR glass fibres. The grid is superficially treated with a coating to facilitate the adhesion with the mortar. The mesh size is 15,7 × 10,1 mm. The coupled mortar is based on a hydraulic binder, containing pozzolanic reactive, selected aggregates, and special additives. The compressive strength of 22 MPa (as provided by the manufacturer) is higher than that of the other mortars used in this investigation.

#H: it is an AR fibre glass grid with a mesh size of 25 × 25 mm. The fibres have been superficially treated with a coating to improve the adhesion with an inorganic matrix. The FRCM reinforcement was made with a mortar based on natural hydraulic lime (Type m-H). The manufacturer provides a compressive strength and a Young's modulus of 15 MPa and 8 GPa, respectively.

The tested materials, while having a great variability, almost completely cover the existing products available on the market. In fact, the yarn spacing of the grid varies from a minim value of 7,6 mm (#D) to a maximum of 99 mm (#B-99); the tensile strength of the utilized fibres (in all case AR glass fibres) ranges from 900 MPa to 1700 MPa. Also the mechanical proprieties of the mortar vary in a broad range: from 5 MPa for m-A mortar to a >25 MPa for m-B3. The mentioned variability involved a remarkable difficulty in the analysis and comparison of both tensile properties of FRCM systems and their interface behaviour with the masonry substrates; on the other hand a broad results spectrum is provided that furnishes a useful database and interesting

Table 1
Mechanical and geometrical properties of textile (fibre grids).

Grid designation	A	B-33	B-66	B-99	C	D-1	D-2	E	F	G	H
Type of glass fibres	Alkali-Resistant (AR)										
Nominal Area (mm^2)	–	3,8[a]	3,8[a]	3,8[a]	–	–	–	–	–	–	35,27[b]
Equivalent thickness (mm)	0,04	–	–	–	0,072	0048	0,046	0,05	0,031	–	0,035
Weight per area (kg/m^2)	0,22	1,00	0,50	0,35	0,32	0,20	0,22	0,25	0,36	0,36	0,23
Grid spacing (mm)	15 × 15	33 × 33	66 × 66	99 × 99	12 × 12	15 × 15	7,6 × 7,6	–	10 × 12,5	15,7 × 10,1	25 × 25
Tensile strength along fibre direction (MPa) (f_t)	1700	921[d]	921[d]	921[d]	>1400	1300	1300	>2000	1600	–	1275
Young's modulus (GPa)	72	23[e]	23[e]	23[e]	74	65	65	70	80	–	72
Failure load single roving (kN)		3,5	3,5	3,5	–	–	–	46[c]	49[c]	77[c]	45[c]
Failure strain (%)	3	1,5	1,5	1,5	2	2,5	2,5	>3,0	2	4,1	1,8

[a] According to [32].
[b] Area per unit length in mm^2/m.
[c] Failure load in kN/m.
[d] Indirectly obtained by the data sheet and referring to the net area of fibres.
[e] Reported in the data sheet as equivalent tensile elastic modulus.

Table 2
Mechanical properties of the mortars.

Mortar designation	m-A	m-B1	m-B2	m-B3	m-C	m-D	m-E	m-F	m-G	m-H
Compressive strength (MPa)	5÷15	>8	8	>25	≥6,5	18	>15	>15	22	>15
Flexural strength (MPa)	–	1,0	1,0	2,0	≥3	–	–	>5	6	–
Compressive elastic modulus (GPa)	–	<8,0	<8,0	<20	–	16	–	9,0	7,6	8,0
Binder[a]	L	L	LC	LC	L	L	L	L	L	L

[a] L = Lime; LC = Lime and Cement.
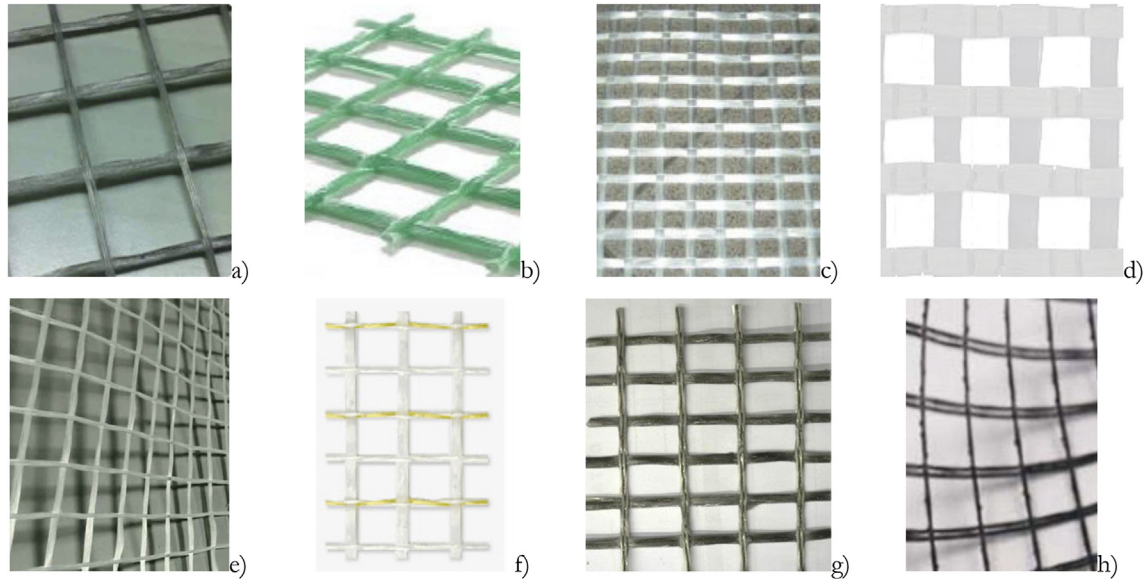
Fig. 1. Glass Grid: (a)#A; (b)#B-33/66/99; (c)#C; (d) #D1-2; (e)#E; (f)#F; (g)#G; (h)#H.

Table 3
Review of the tested materials.

FRCM type	Lab	Reinforcement (Textile)	Mortar
#A	Polimi	A	m-A
	ZAG		
#B-1	Unisalento	B-33	m-B1
#B-2	Unipg	B-33	m-B2
	Units		
#B-3	Unisalento	B-66	m-B3
	Uminho		
#B-4	Unipg	B-66	m-B2
	Units		
#B-5	Unisalento	B-99	m-B3
#B-6	Units	B-99	m-B2
#C	Cut	C	m-C
	Unibo		
#D-1	Unisalento	D-1	m-D
#D-2	Unipd	D-2	m-D
#E	Unirm3	E	m-E
	Upatras		
	Unipd		
#F	Uminho	F	m-F
	Unibo		
	Unifi		
	Unipd		
	Unirm3		
#G	Aachen	G	m-G
	Polimi		
	ZAG		
#H	Unina	H	m-H
	Unisannio		

indications concerning both the mechanical characterization and the test procedures; finally the obtained results may be very useful to address the future research developments.

3. Tensile tests

3.1. Specimens and test set-up

The tensile tests were first performed on FRCM specimens in order to obtain the stress-strain curve and the main mechanical properties of each composite. Tensile tests were carried out in all the 15 laboratories involved in the research activity, using common specifications according to the test arrangement shown in Fig. 2. All types of glass fibre grids have been included in the experimental campaign and 125 prismatic specimens with rectangular cross-section were tested. Specimens were cast at each laboratory or furnished by the supplier using either a single mould for each specimen or cutting the specimens from a large plate. Although in the present Round Robin common guidelines have been agreed and basically observed, the variability of the used materials has led in some cases to the realization of samples with different sizes and to the variation of gripping systems and experimental set-ups. In addition, at the University of RWTH Aachen the specimens were tested according to [69]. The geometrical details of the tested specimens are listed in Table 4; each laboratory tested at least five specimens for each product.
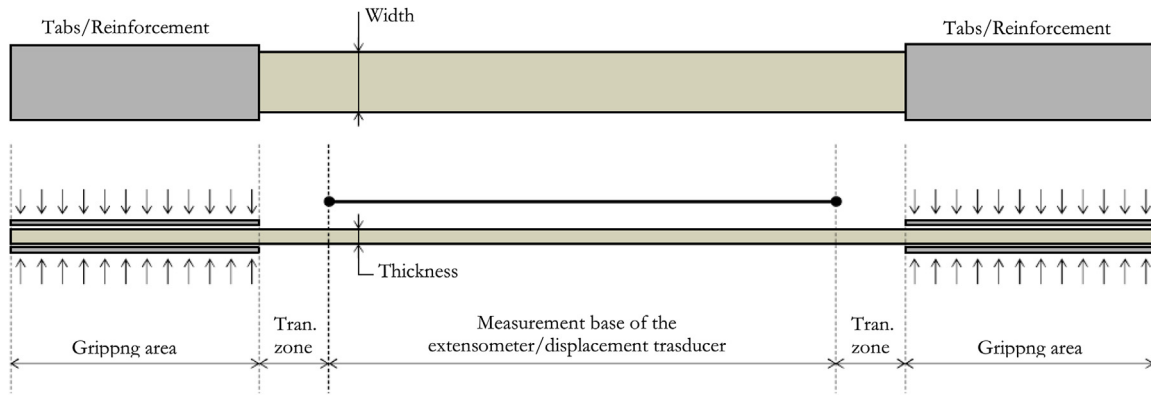
Fig. 2. Tensile test arrangement.

Table 4
Geometrical details of specimens.

FRCM type	Labs	Thickness (mm)	Width (mm)	Length (mm)	Dry cross-section (mm²)	Clamping system	Test age (days)
							Curing conditions
#A	ZAG	9	50	400	2,4	The ends are treated with epoxy. Clamping was done without tabs	–
	Polimi	9	50	400	2,4	GFRP tabs	50
							T = 20°C- 50% RH
#B-1	Unisalento	12	100	260	11,4	CFRP tabs	60–120
							T = 20°C- 50% RH
#B-3	Unisalento	30	130	900	7,6	CFRP tabs	194
							T = 20°C- 100% RH for 59 days
							T = 25 °C for 135 days
#B-4	Unipg	30	130	–	7,6	CFRP tabs	120
	Units	30	130	900	7,6	CFRP tabs	77
							T = 23°C- 100% RH for 59 days
							T = 25 °C for 18 days
#B-5	Unisalento	30	200	900	7,6	CFRP tabs	209
							T = 23°C- 100% RH for 59 days
							T = 25 °C for 150 days
#B-6	Units	30	200	900	7,6	CFRP tabs	78
							T = 23°C- 100% RH for 30 days
							T = 25 °C for 48 days
#C	Unibo	6	60	500	3,6	CFRP tabs	153
							T = 20 °C
	Cut	6	60	500	3,6	GFRP tabs and rubber pads clamped with two bolted plates	–
#D-1	Unisalento	12	100	260	3,6	CFRP tabs	60
							T = 23°C- 50% RH
#D-2	Unipd	14	40	400	1,5	Steel tabs glued on the specimens and connected with pin	60
							T = 21°C- 68% RH
#E	Upatras	10	75	500	3,8	CFRP tabs	49
							T = 20°C- 65% RH
	Unirm3	10	50	600	2,3	GFRP tabs	110
							48 h wet; 26 days in water,
							T = 22°C- 60% RH for 72 days
#F	Unirm3	10	40	500	1,4	GFRP tabs	–
	Unifi	10	40	400	1,4	Aluminium tabs	142–162
	Unipd	11	40	399	1,4	Steel tabs glued on the specimens and connected with pin	–
	Uminho	10	40	400	1,4	Aluminium tabs	–
	Unibo	10	40	400	1,4	FRP tabs	150
							T = 20 °C
#G	RWTH-Aachen-1	10	60	500	2,7	no tabs	31
							T = 20°C- 100% RH
	RWTH-Aachen-2	10	60	1000	2,7	no tabs	38
							T = 20°C- 100% RH
	Polimi	10	55	420	2,7	GFRP tabs	50
							T = 20°C- 50% RH
#H	Unina	10	100	600	3,5	GFRP tabs	56
	Unisannio	10	100	500	3,5	GFRP tabs	130
	Uminho	–	–	–	–	Aluminium tabs	–

All laboratories used a universal testing machine; tests were carried out under displacement control at a rate ranging between 0,1 and 0,3 mm/min, up to the failure. Specimens were provided with fibre-reinforced polymer (FRP), steel and aluminium tabs or FRP wrap at the ends in order to avoid any damage within the gripping systems and to guarantee an effective load transfer from

the testing machine; only in the case of test performed at the RWTH the ends of the specimens were not strengthened [68], while at ZAG a simple layer of epoxy resin was utilized. The configuration used for the specimen ends for each lab is summarized in Table 4. Although it is known the possible influence of this aspect on the experimental results [28,70], it was not specifically focused in the present paper. However an in-depth analysis concerning the effects of ends configurations is suggested for the future progress of the research.

Displacements and axial strain were recorded. To measure the displacements, most of the laboratories used extensometers directly connected to the FRCM specimen; in few cases potentiometers and optical methods (digital image correlation) were utilized.

A data acquisition frequency not less than 5 Hz was used to guarantee sufficient informations in case of brittle phenomena.

Test results are given in terms of tensile strength, ultimate strain and elastic modulus. Fig. 3 shows a typical stress-strain curve for a FRCM material, where the tensile stress can be calculated referring to the area of the dry textile. The curve can be assumed as tri-linear: the first branch represents the un-cracked stage and its slope E_1 effectively provides the Young's modulus of the whole FRCM composite material (mortar + fibers); the second branch corresponds to the post first crack formation stage (the slope being E_2). At this phase, following the starting of the mortar cracking, a reduction of the composite stiffness is expected as well as a further evolution of the cracking. The first and second stage are governed by the mechanical properties of both mortar and fibre grid as well as by their interface properties. Finally, the third phase basically corresponds to the tensile behaviour of the grid and it is characterized by the slope E_3. At this last stage the matrix results completely damaged and doesn't contribute to bear the applied load, the number of cracks is stabilized and any load increment only widens the existing ones; it should be mentioned that the third stage in some cases wasn't observed, depending mainly on the contribution of the tension stiffening effect and on the tensile strength of the fibres.

The obtained experimental results are discussed in the following in terms of: first cracking strength σ_{t1}, defined as that value of stress at which the stress strain curve shows an apparent variation of the slope due to the starting of the matrix cracking; the ultimate strength, σ_u, defined as the stress at failure; the first modulus E_1 that corresponds to the slope of the un-cracked phase; the modulus E that represents the slope of the segment joining the points characterized by the stress values σ_{t1} and σ_u and it is representative of the stiffness at the cracked phase. This last choice follows to the need of a more homogeneous analysis of results since the experimental curves show, in some cases, a large scatter and the last two stages (see Fig. 3) cannot clearly identified. Therefore, as reported in the next section, only two phases are identified in all cases: the un-cracked phase and the cracked/cracking phase. In other words the second and third stage are combined in a unique one, including the possible evolution of cracking phase and the completely cracked situation up to the failure [65–67].
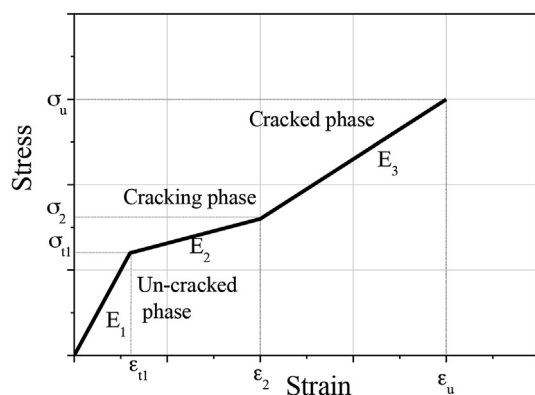
Fig. 4 shows the pictures of the various test set-ups.

3.2. Test results

As expected the tensile strength of Glass FRCM specimens is manly governed by the glass fibre strength and by the interface performance between the fibers and the inorganic matrix. Fig. 5 shows the three different failure modes observed during the tensile tests. Special attention should be paid to failure mode "A" as it occurs prematurely near the gripping devices; this crisis is due to a biaxial stress state at the area near the grips because of the simultaneous compression action of the gripping clamps and the applied tensile load; the mentioned occurrence may cause a significant underestimation of the tensile strength of the FRCM material. Failure modes B or C are caused by the glass fibres rupture or the mortar cracking and the subsequent fibres slippage within the inorganic matrix, respectively.

Failure of some specimens is shown in Fig. 6. Specimens did not fail suddenly after the first crack of the mortar and, hence the glass mesh properties and/or the interface between mortar and reinforcement are involved. The fibre arrangement inside the FRCM grid (Fig. 7), comprised of braided yarns along the two (weft and warp) directions, makes the longitudinal fibres not straight after cast causing a in some cases a no-uniform distribution of the load during the test.

Experimental results are listed in Table 5 in terms of stiffness values (E_1, E, i.e. referred to un-cracked and cracked phase, respectively), stresses (σ_{t1}, σ_u) and strains (ε_{t1}, ε_u); the table also reports the failure mode. The parameters have been calculated using the dry glass fibre cross-sectional area, as given in the manufacturer data sheet; the Coefficients of Variation (CoVs) are also provided. In addition, the ratio of the experimental value of modulus E to the nominal elastic modulus (E_{nom}) and the ratio between the ultimate strength, σ_u and the tensile strength of the fibres (f_t) are reported; the values E_{nom} and f_t are those furnished by the manufacturer (see Table 1).

A comparison of the results is made in terms of the most significant parameters characterizing the tensile behaviour of each material tested. However, by analysing the CoV values, a large dispersion of the data (CoV higher than 15%) can be observed in some cases. Only for the tensile strength (σ_u) the data referred to a specific FRCM system seem to be in fair agreement between different labs and also less scattered as concerns results referred to the same laboratory. This is because the ultimate phase of the response is most likely governed by the glass fibre tensile strength and the contribution of the mortar is negligible. It is worth noting that the ultimate strength (σ_u) is always lower than the nominal tensile strength of the fibres (Table 1); these results are probably due to the fact that in the FRCM composite material, especially after the cracking of the matrix, even if a uniform distribution of the load between the different rovings of the grid is expected, a variation in the axial load of each fibre belonging to the same bundle may occur [60,69]. This phenomenon may lead to additional flexural stresses in some rovings that in turn resulted more loaded than others. Conversely, the values obtained for ratio E_3/E_{nom} suggest that in most cases the slope of the cracked phase could be effectively related to the stiffness of the fibres alone. In some cases, E_3 is greater than the E_{nom}; this result could be attributed to the

Fig. 3. Typical stress-strain curve.
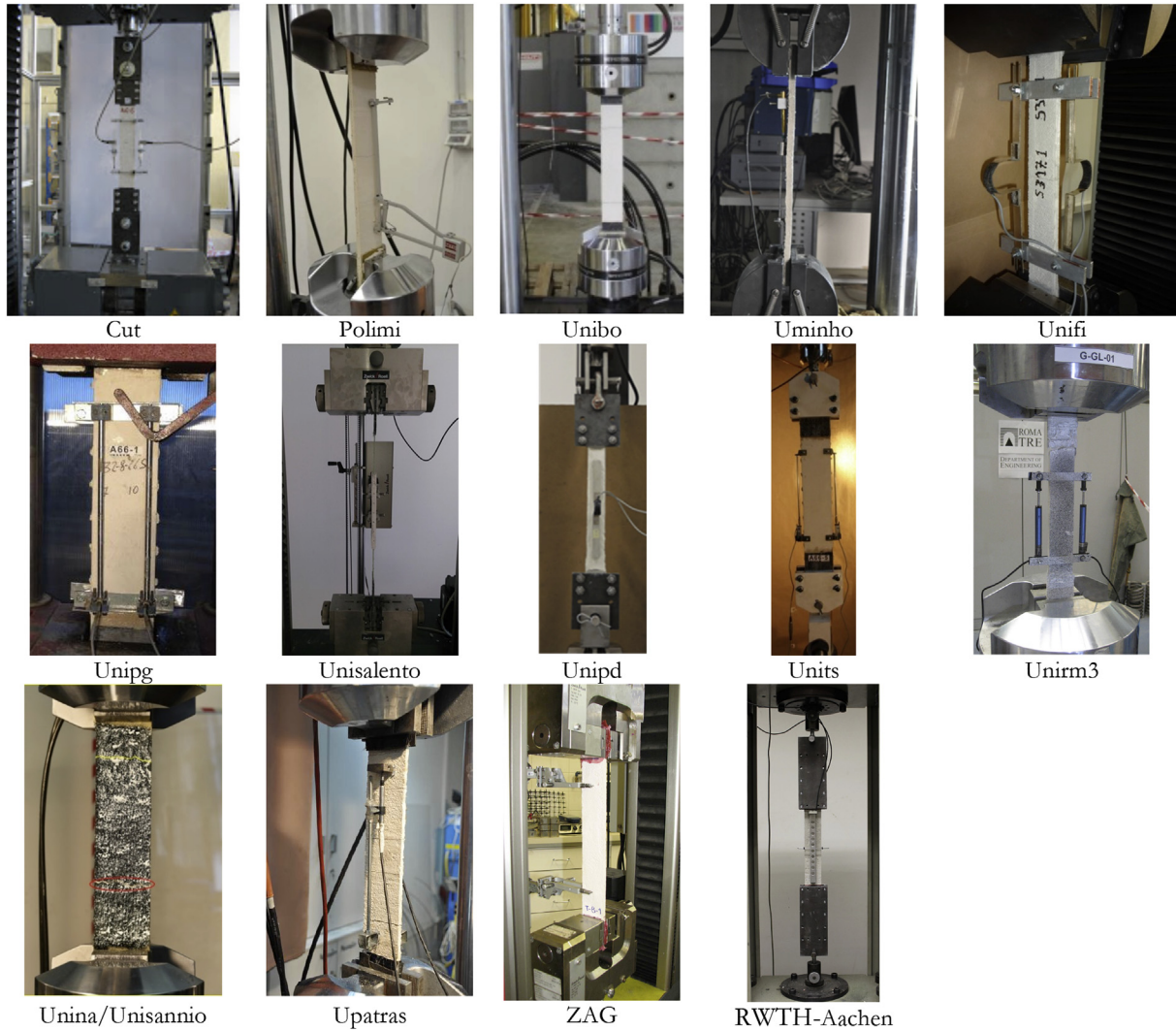
Fig. 4. Test set-ups.
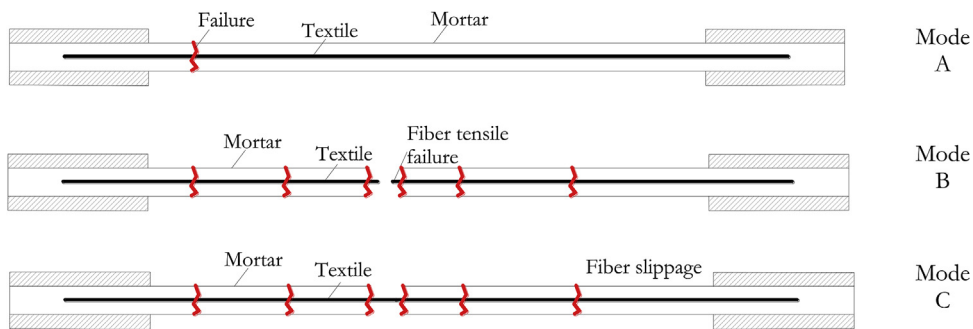
Fig. 5. Failure modes (tensile test).

dispersion of the experimental data but also to the tension stiffening effect of the mortar; in fact the evaluation of E (as better detailed above) refers to the whole phase following the first cracking of the mortar.

In addition, the experimental data are compared in terms of stress-strain curves and, when available, the straight line, passing through the origin of the axes and with a slope equal to the Young's Modulus of the textile is marked in the drawing. This allows to

graphically identify the difference between the tensile behaviour of the composite and that of the fibre grid alone and to better appreciate the tension stiffening contribution of the mortar.

The mentioned comparison between stress-strain curves are reported only when test made at least in two labs are available, thus the reinforcement #B-1, #B-3, #B-5 and #B-6 have been excluded as tested only by one lab.

For FRCM with type #A grid, tests were carried out at two
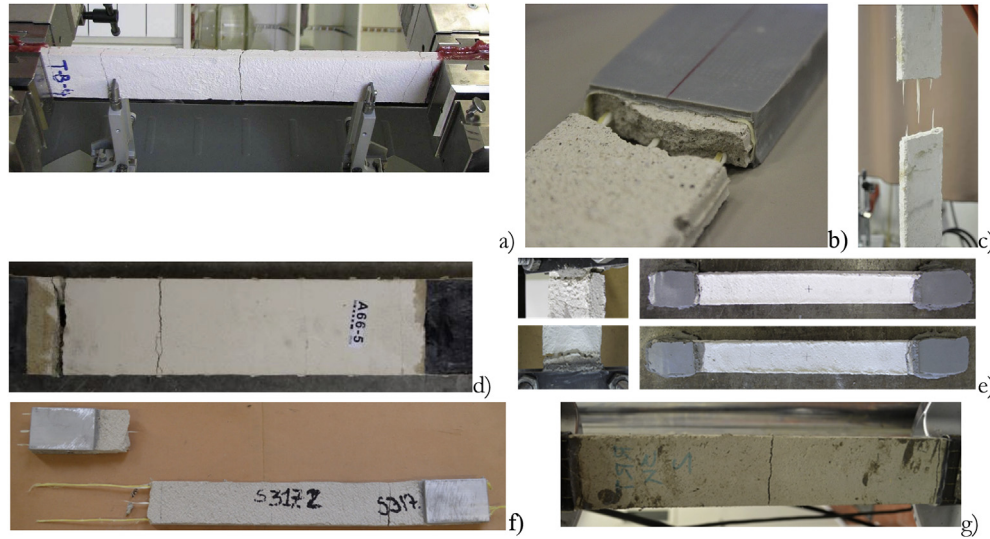
Fig. 6. Mode of failures: (a) Mode C − ZAG - #A; (b) Mode A − Unibo - #F; (c)Mode B − Upatras- #E; (d) Mode B − Unipg - #B-4; (e) Mode C − Unipd - #D; (f) Mode A + C − Unifi - #F; (g) Mode B − Polimi - #G.
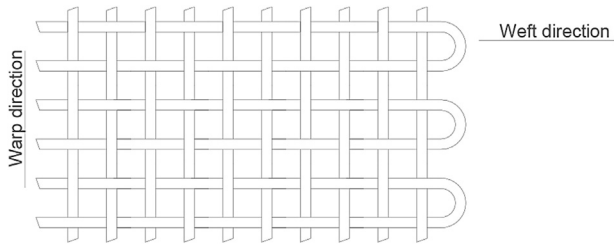
Fig. 7. Typical grid configuration.

different laboratories (Zag and Polimi). A high scatter can be noted by comparing the results obtained by the two labs (Table 5 and Fig. 8a); only the deformations at the first cracking (ε_{t1}) appear

similar. The cause could be attributed to the presence of micro-cracks detected along the specimens by the ZAG lab before testing.

It is worth noting that type #B grids were pre-impregnated by a thermosetting epoxy vinylester resin: this entails for a different mechanical behaviour compared to that of other types of mesh. For this type of material, the comparison was made only for #B-4 specimens which were tested at two labs (Unipg and Units). The CoV values range between 7 and 44%. For this system the difference between the values measured at Unipg and Units is substantial except for the ultimate strength value for which the difference is around 1%. Fig. 8b reports the comparison in terms of stress-strain behaviour. Despite of the quantitative scatters already discussed the trend of the curves appears to be similar. In particular, a pro-gressive cracking of the mortar can be noticed after the first

Table 5
Tensile tests: results.

FRCM type	Lab	E_1 (GPa)	COV (%)	σ_{t1} (MPa)	COV (%)	ε_{t1} (%)	COV (%)	E (GPa)	COV (%)	σ_u (MPa)	COV (%)	ε_u (%)	COV (%)	E/E_{nom} (%)	σ_u/f_t (%)	Failure mode
#A	ZAG	345	34	74	20	0,034	48	60	35	369	7	0,69	20	83	22	C
	Polimi	1111	35	428	21	0,037	46	79	10	611	21	0,49	26	110	37	B
#B-1	Unisalento	120	1	48	21	0,020	8	92	9	1535	11	1,62	37		167	–
#B-3	Unisalento	506	16	708	24	0,130	22	162	26	1318	13	0,84	25		143	A
#B-4	Unipg	988	44	205	30	0,030	55	93	10	1349	15	1,45	14		146	A-B
	Units	3922	10	365	7	0,094	14	59	26	1338	7	1,84	22		145	B
#B-5	Unisalento	377	40	1175	42	0,330	56	149	8	1476	4	1,08	23		160	B
#B-6	Units	5576	3	662	2	0,012	15	9	33	956	10	2,69	7		104	C
#C	Unibo	236	19	125	6	0,055	20	70	5	1165	3	1,54	2	95	83	B
	Cut	283	11	128	6	0,041	12	64	5	1294	3	1,75	9	86	92	B/A
#D-1	Unisalento	85	12	254	1	0,300	13	66	6	325	8	0,47	6	102	25	C
#D-2	Unipd	1226	51	186	30	0,019	67	36	9	438	16	1,02	17	55	34	C
#E	Upatras	1399	21	722	26	0,060	13	53	30	1221	20	1,38	36	76	61	B
	Unirm3	1592	10	496	23	0,050	10	52	23	1242	5	1,58	6	74	62	A
#F	Unirm3	1480	9	626	7	0,049	6	119	3	2163	4	1,42	11	149	135	A
	Unifi	3359	45	404	65	0,014	33	113	44	971	14	1,03	41	141	61	A-C
	Unipd	1783	81	528	15	0,044	117	75	70	800	8	0,66	55	94	50	C
	Uminho	1376	78	774	22	0,396	70	–	–	1289	7	0,60	142	–	81	C
	Unibo	5333	7	852	18	0,019	19	95	44	1252	18	1,54	39	119	78	A-C
#G	RWTH-Aachen-1	3030	3	733	37	0,025	13	75	25	882	12	0,45	17	–	–	A
	RWTH-Aachen-2	3281	11	525	25	0,015	11	68	14	992	6	1,26	19	–	–	A
	Polimi	1742	29	633	26	0,044	37	73	11	1157	18	1,23	15	–	–	B
#H	Unina	2751	10	680	7	0,079	28	51	16	807	3	0,93	31	71	63	C
	Unisannio	1353	36	658	16	0,070	25	30	12	900	6	1,03	21	42	71	A
	Uminho	703	24	550	15	0,052	12	–	–	680	25	0,19	46	–	53	C
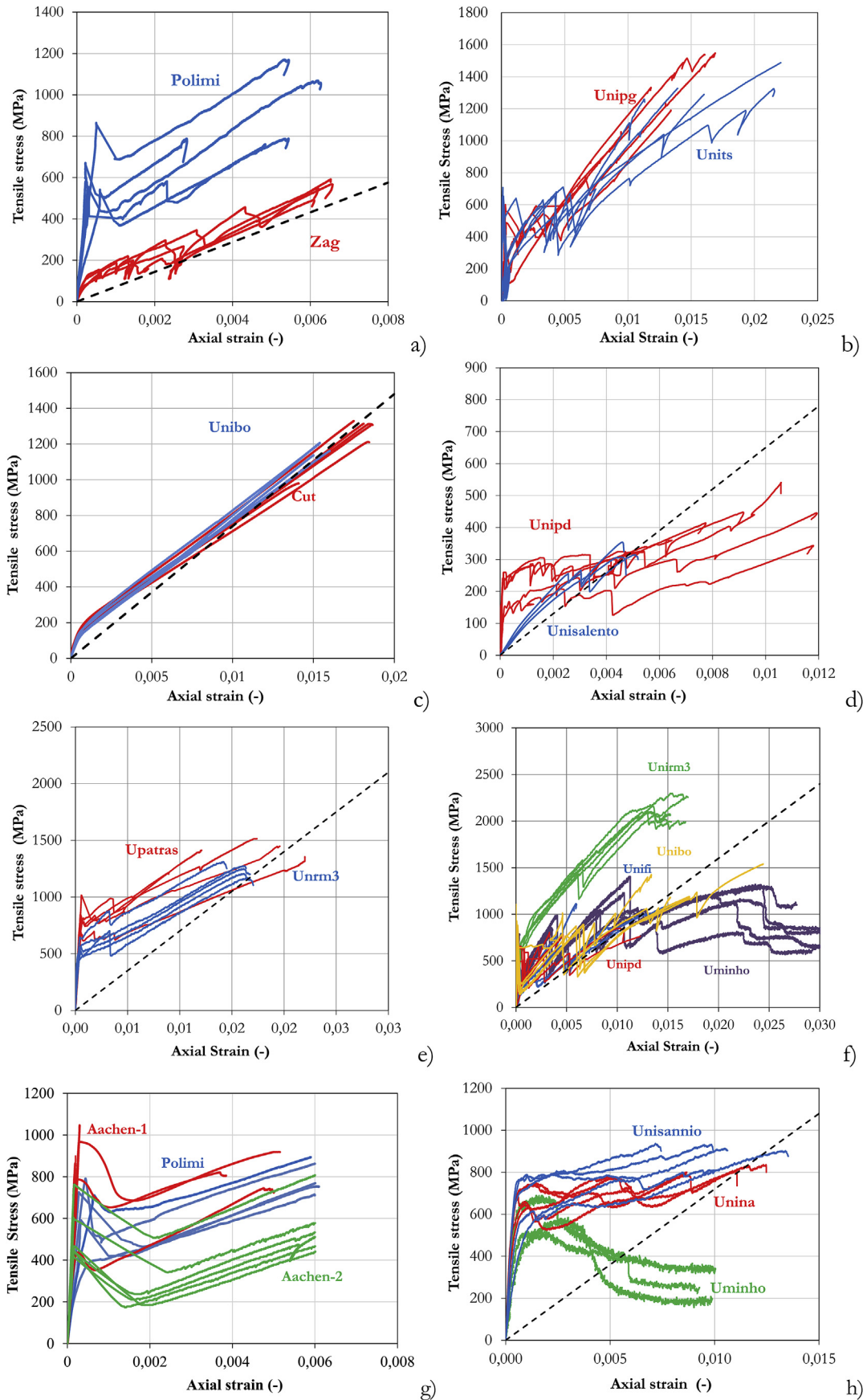
Fig. 8. Stress strain behaviour:(a)#A (b)#B-4; (c) #C; (d)#D; (e)#E; (f)#F; (g)#G; (h)#H.

cracking strength is attained, followed by a hardening behaviour.

The tests performed at Unibo and Cut on #C type reinforcement showed a good level of repeatability for all parameters investigated (CoV between 5% and 19%). The results are also comparable between the two laboratories. In addition, the stress versus strain curves are similar. Moreover, for this composite load drops usually due to cracking phenomena in the matrix are not visible.

Mortar cracking and slippage between the textile and the mortar were observed for tests on type #D reinforcement carried out at Unisalento and Unipd laboratories. The ultimate strength values varied from 325 (CoV = 8%) to 438 MPa (CoV = 16%) passing from #D-1 to #D-2 reinforcement. The other mechanical parameters (E_1, σ_{t1}, ε_{t1}, E_3 and ε_u) are also quite different (Table 5 and Fig. 8d), The observed difference could be reasonably related to the strands spacing of reinforcing mesh (15 mm for #D-1 and 7,6 mm for #D-2), the different tensile set-ups (samples directly clamped into the testing machine for Unisalento and clevis-type grips for Unipd) and the sample ends preparation (CFRP tabs at Unisalento and steel tabs at Unipd).

Tests on the FRCM system with type #E fibres were conducted at Unirm3 and Upatras laboratories. The mechanical parameters and the stress-strain curves obtained by the two laboratories − Table 5 and Fig. 8e - are similar. The average ultimate strength and strain were 1232 MPa and 1,49%, respectively. Results in terms of the parameter E_1 were also consistent (1399 MPa at Upatras and 1592 MPa at Unirm3), as well as the values of ε_{t1} (0,060 at Upatras and 0,050 at Unirm3). In terms of first cracking stress, a significant scatter has been found comparing results of the two labs, in all cases several load drops can be observed in the experimental curves corresponding to the cracking evolution within the mortar.

The experimental results regarding type #F GFRCM are characterized by relevant differences, Fig. 8f. As all specimens were prepared by the supplier following the same procedure, the only objective difference is related to the ends sample preparation at the involved labs: FRP tabs were used at Unirm3 and Unibo, aluminum tabs at Unifi and Uminho while steel tabs were used at Unipd. . The ultimate tensile strength recorded at Unirm3 is very high if compared to the values found at the other labs; by averaging all the results and excluding those of Unirm3 it is possible to estimate a tensile strength of 1078 MPa (CoV = 22%). Only the first cracking stresses are similar for all laboratories (including Unirm3) and the average value is approximately 640 MPa (CoV = 33%). The relevant different behaviour registered also in terms of stress-strain curves suggests the need of further investigations devoted to a deeper understanding of the influence of boundary conditions on tensile test results (Fig. 4).

The tensile behaviour of #G FRCM system was investigated at RWTH-Aachen and Polimi. From Table 5, it is possible to note that the data are comparable between the laboratories in terms of ultimate strength, while different values have been recorded for the corresponding ultimate strain. The average value of the first cracking stress was 630 MPa (COV = 17%) while that of the tensile strength was 1010 MPa (COV = 14%). The comparison in terms of stress-strain behaviour is reported in Fig. 8g, where the curves referring to RWTH-Aachen-2 aren't drawn up to the ultimate strain aiming to improve the graphical representation. Even if the scatter among data are confirmed by analysing the mentioned Figure, the slope of the second stage of the curves appears similar.

Results on grid type #H highlight again some differences among different laboratories. While the ultimate strength recorded at Unisannio was 900 MPa, an ultimate strength equal to 680 MPa was obtained at Uminho; this scatter is probably due to the large mesh size that makes the reinforcement more sensitive to the possible misalignment of the rovings with respect to the tensile load direction. Test results in terms of first cracking strength σ_{t1} are similar and in the range of 550−680 MPa, the variability in this case can be linked to the different cracking evolution within the grout. The analysis of the stress-strain curves is reported in Fig. 8h, where it can be noted that the stress-strain responses for the test performed at Unisannio and Unina are very similar. An almost horizontal branch is recognizable after mortar cracking (intermediate phase) probably associated with significant slips between mortar and fibres. After such a phase, the behaviour of the composite tends again to a linear trend (third stage) with a slope sensibly lower than the nominal modulus of dry textile; this last found could be attributed to the slip phenomena occurring between the glass grid and the mortar and the consequent uneven distribution of tensile load among the five glass rovings. On the other hand the shape of the stress-strain curve recorded at Uminho is quite different, especially concerning the post peak branch, characterized by a softening behaviour that would lead to deduct a premature failure.

3.3. Tensile test results: experimental comparison

As discussed in section 3.2, test results are characterized by a low level of repeatability especially when referring to the first stage (before mortar cracking), this makes difficult a rigorous analysis able to catch the influence of the two components (mortar and fibres) and their interface on the tensile behaviour of FRCM systems. However it may be well recognized that before mortar cracking in all cases the tensile behaviour is governed by the combination of the components properties (mortar and reinforcement), whereas with the formation of the first cracks in the mortar the interaction between reinforcement and matrix and the mechanical properties of the reinforcement play a significant role. The results obtained furnish a wide database that represents a relevant contribution to this almost unexplored topic and highlight also some critical aspects useful to address the future research works. Regarding the strength evaluation, it is suggested to define an equivalent cross-sectional area for the analysis of the first phase, namely before the mortar cracking, in order to more realistically include the contribution of the mortar; while in the second stage it is possible to refers to the area of the dry fibres reinforcement alone.

In addition, in the authors' opinion the relative distance between the cracks and the fixing points of the instruments used to measure the strains may highly affect the registered data. To avoid this sensitivity, the gage length should be quite large and comparable with the distance between the specimen tabs.

The comparison between the results obtained for different materials in terms of both first cracking and ultimate stress is shown in Figs. 9 and 10 for the FRCM coupons herein presented. Each plot reports the experimental points, the mean value (dashed line) and the corresponding standard deviation (hatch area). Fig. 9 refers to fibres superficially treated with a coating to improve the adhesion with mortar, while Fig. 10 refers to glass fibres without bonding agent. Test results for coated fibres are less scattered and it is possible to estimate a reliable value of the ultimate stress: σ_u = 1160 MPa (CoV = 15%). The first cracking stresses show a high variation, σ_{t1} = 497 MPa (CoV = 56%), confirming that in this case a more appropriate definition of geometrical dimensions (i.e. dimensions of the cross section) should be considered. On the contrary, the results found for FRCM specimens cast without a bonding agent are more scattered (Fig. 10): σ_u = 767 MPa (CoV = 42%) and σ_{t1} = 487 MPa (CoV = 50%). It is clear as the addition of the bonding agent may increase the level of composite action in terms of collaboration between the fibres and the mortar, but could involve a reduction of fire and heat resistance of the composite material depending on the amount of added polymer.
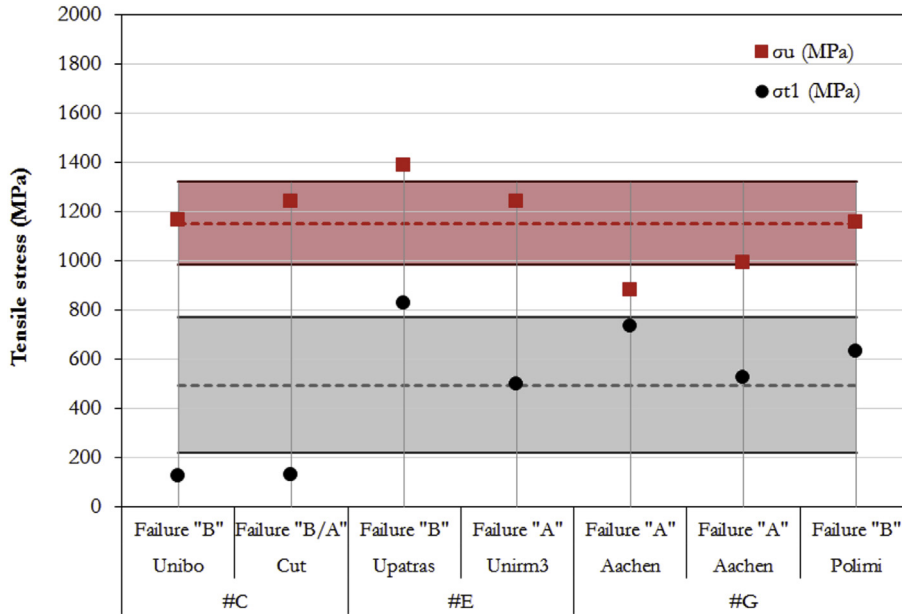
Fig. 9. Experimental comparison – GFRCM with coating.

3.4. Bond tests

In order to study the load transfer mechanisms and the bond strength of FRCM reinforcement bonded to brick masonry surfaces, 130 FRCM/masonry specimens were prepared and tested under shear.

3.5. Specimens and test set-up

The masonry substrate was constructed using "San Marco Rosso Vivo A6R55W" solid clay bricks and a mortar classified as M5 or lower according to [70]. The masonry prisms were made by stacking together 5 bricks with 10 mm thick mortar joints; their nominal dimensions are listed in Table 6. The compressive strength of the brick is 14,8 MPa, the tensile strength is 2,5 MPa while the elastic modulus is 5760 MPa, according to [29]. The different FRCM

reinforcements were made by using the same glass fibre grids and mortars described for tensile tests and, correspondingly, they will be referred to in the following with the same nomenclature.

The test setup was a single-lap shear test with the exception of tests carried out at ZAG where a double-lap configuration was used. According to Table 6, the bonded length was 260 mm; different bonded lengths, ranging from 120 to 260 mm were tested only for reinforcement of type #B. The bonded width varied between 30 and 132 mm. For specimens tested at Unisalento, the dry glass textile at the un-bonded length (i.e. between the loaded end and the grip) was impregnated with an epoxy resin with the aim of improving the stress distribution.

All laboratories, with the exception of Unibo (for FRCM type #C) and Unisannio, used a universal testing machine to apply the load. In the cases of the tests performed at Unisalento, Zag, Polimi, Units, Uminho, Unibo (for FRCM type #F) Upatras, Unifi, Unipd and Unina
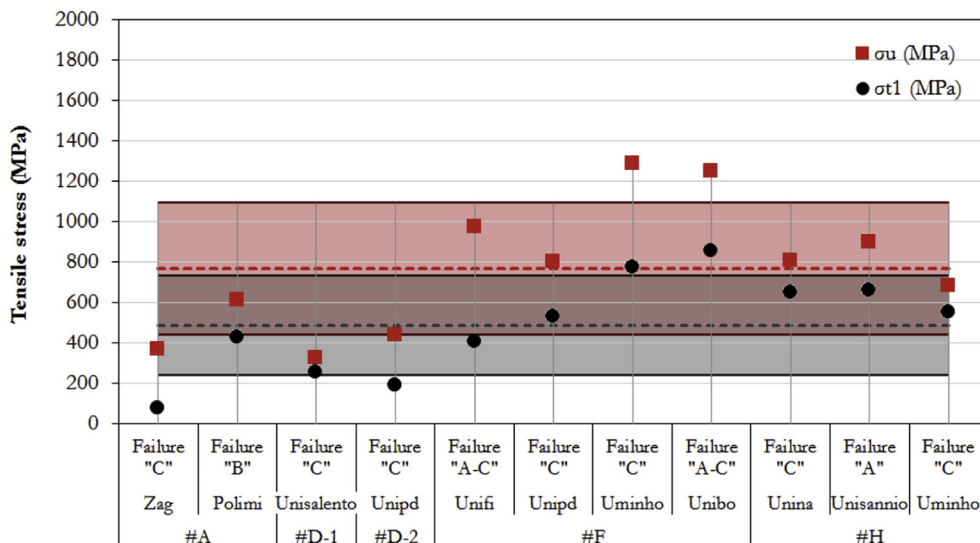
Fig. 10. Experimental comparison – GFRCM without coating.

Table 6
Geometrical details of the specimens (bond tests).

FRCM type	Lab	Brickwork substrate			Bond area	
		Thickness [mm]	Width [mm]	Height [mm]	Length [mm]	Width [mm]
#A	Zag	55	120	310–315	265	100
	Polimi	120	250	300	260	100
#B-1	Unisalento	120	250	320	260	100
#B-2	Unipg	120	250	315	240	131
	Units	120	250	315	240	132
#B-3	Uminho	–	–	–	120	30
		–	–	–	180	30
#B-4	Unipg	120	250	315	120	131
	Units	120	250	315	240	132
#C	Unibo	120	125	315	260	60
	Cut	120	250	315	260	60
#D-1	Unisalento	120	250	320	260	100
#D-2	Unipd	120	120	310	260	40
#E	Upatras	125	250	325	260	75
	Unirm3	120	125	310	260	50
	Unipd	125	125	315	260	75
#F	Unirm3	120	125	310	260	40
	Unifi	120	123	315	260	40
	Unipd	120	120	310	260	40
	Uminho	–	–	–	260	40
	Unibo	125	125	315	260	40
G	Zag	120	250	300	260	100
	Polimi	120	250	300	260	100
#H	Unina	120	200	320	260	125
	Unisannio	120	250	315	260	125
	Uminho	–	–	–	260	100

the specimens were placed on a steel frame support mechanically connected to the testing machine. The steel plates used were machined to reduce misalignment effect, this general loading configuration is shown in Fig. 11a—b.

The FRCM/masonry joint was loaded in shear by applying a tensile load to the FRCM strip; the strip end was reinforced by tabs similar to those employed for tensile testing. The application of the load produced a shear stress at the interface and a compressive and flexural stress state into the brick masonry assemblage.

For specimens tested at Unibo and Unisannio, a purposely designed single-lap set-up was used for bond tests, made of a rigid horizontal frame with front and lateral steel reaction elements utilized to prevent horizontal and vertical displacements, Fig. 11c.

Two types of slippage have been generally measured and recorded: fibres-substrate *(f-s)* and mortar-substrate *(m-s)*. In particular, (m-s) slip was recorded at Unisalento, Units and Unisannio while (f-s) slip was recorded at the other labs. Displacement transducers fixed on the masonry block with the measuring dipstick placed at the loaded end of the reinforcement (mortar or

fibres) were used. In the case of Unisannio, strain gauges were glued at the central roving of the grid before the application of the matrix and the slip was evaluated as integration of the strains along the bonded length. The distance of the strain gauges from the first bonded section was 20 mm, 80 mm, 140 mm and 200 mm.

Specimens (typically 5 per FRCM system and per laboratory) were tested under displacement control at a rate of 0,1—0,3 mm/min up to failure. The applied load, the displacements and all strain readings were recorded by a digital data acquisition system. Fig. 12 shows images of the test set-ups used in different laboratories.

3.6. Experimental results

In this section, the experimental results are summarized for each type of FRCM reinforcement in terms of maximum force (F_{max}) and corresponding slip (s); the coefficients of variation (CoV) are also reported and referred generally to the data obtained for a specific FRCM system even if tested in different labs. In addition, the tensile strength (σ_f) was determined as the ratio between F_{max} and
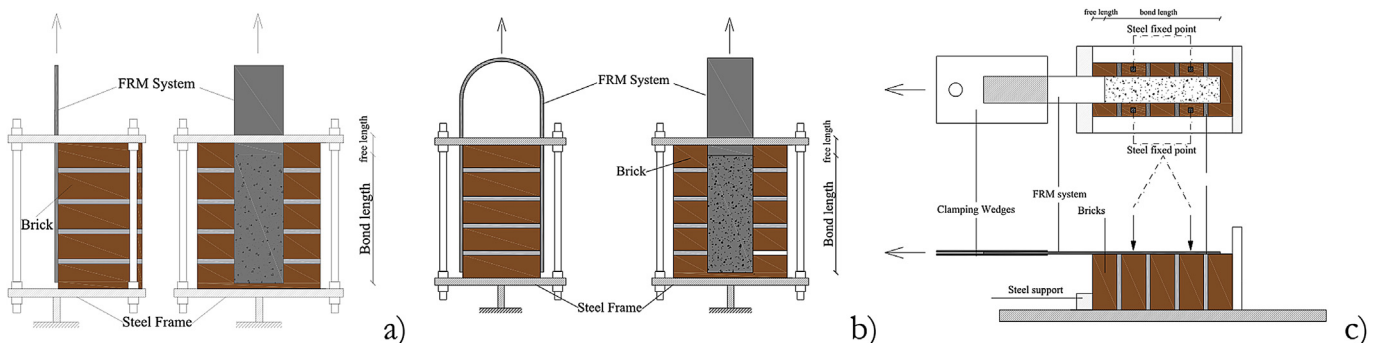
Fig. 11. Bond test arrangement: (a) scheme of the single face shear test set-up; (b) scheme of the double face shear test set-up; (c) test set-up used at the lab of Unisannio and Unibo (for FRCM type #C).
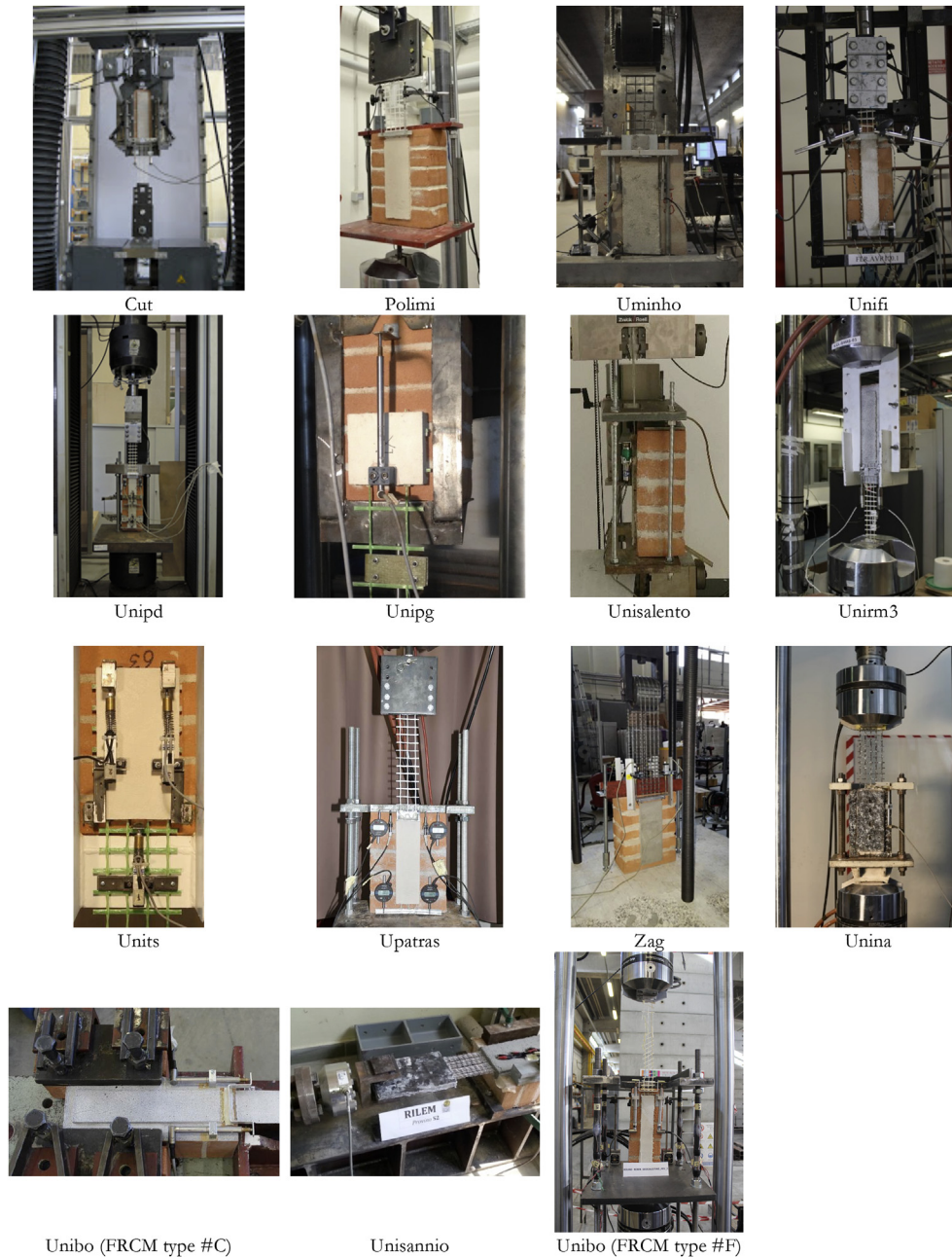
Fig. 12. Bond test set-ups.

the cross-sectional area of the rovings. Finally, the ratio (σ_f/σ_U) was calculated in order to provide an insight to the degree of exploitation of the composite strength when bonded on a masonry substrate and subjected to direct shear. The mode of failure is also discussed according to the failures modes reported in Fig. 13. Six different failure modes have been considered: "Mode A" corresponds to debonding of the reinforcement with a cohesive crisis within the substrate (i.e. part of the substrate remains attached to the debonded FRCM strip); "Mode B" accounts for debonding of the reinforcement with an adhesive failure at the matrix-substrate interface; "Mode C" is associated with debonding of the reinforcement by an adhesive failure at the matrix-fibre interface; "Mode D" corresponds to textile slippage with respect to the mortar; "Mode E" is similar to "Mode D" with the addition of matrix cracking, and finally "Mode F" corresponds to the tensile rupture of

the glass fibres with or without cracking of the mortar. Photos of specimens illustrating typical failure modes are given in Fig. 14.

The results are summarized in Table 7, where the method used to measure the slip at the loaded end by each laboratory is also reported. Analysing the CoVs of the ultimate load values it can be observed that each laboratory obtained consistent results. In fact, in most cases, the CoV are less than 20% and even less than 15%. On the contrary the slip data recorded by each lab are very scattered with a CoV higher than 15% for almost all test results. This scatter is probably linked to the damage/rupture of individual filaments during loading; in fact it is often related to the textiles made by dry rovings while textiles made by impregnated fibres show less scatters. As regards the kind of failure, it should be underlined that the cohesive bond failure within the masonry substrate never occurred; this result highlights the difference between the interface

C. Debonding with cohesive failure of the substrate

A. Debonding at the matrix-to-substarte interface

B. Debonding at the textile-to-matrix interface

F. Textile slippage within the mortar matrix

E. Textile slippage within the matrix with cracking of the outer lever of mortar

D. Tensile rupture of the textile (out of the bonded area)
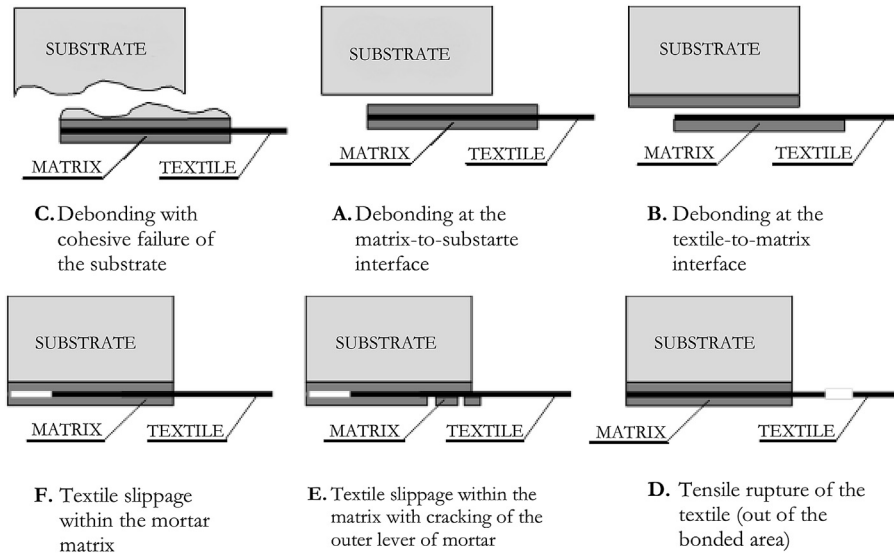
Fig. 13. Failure modes (bond tests).
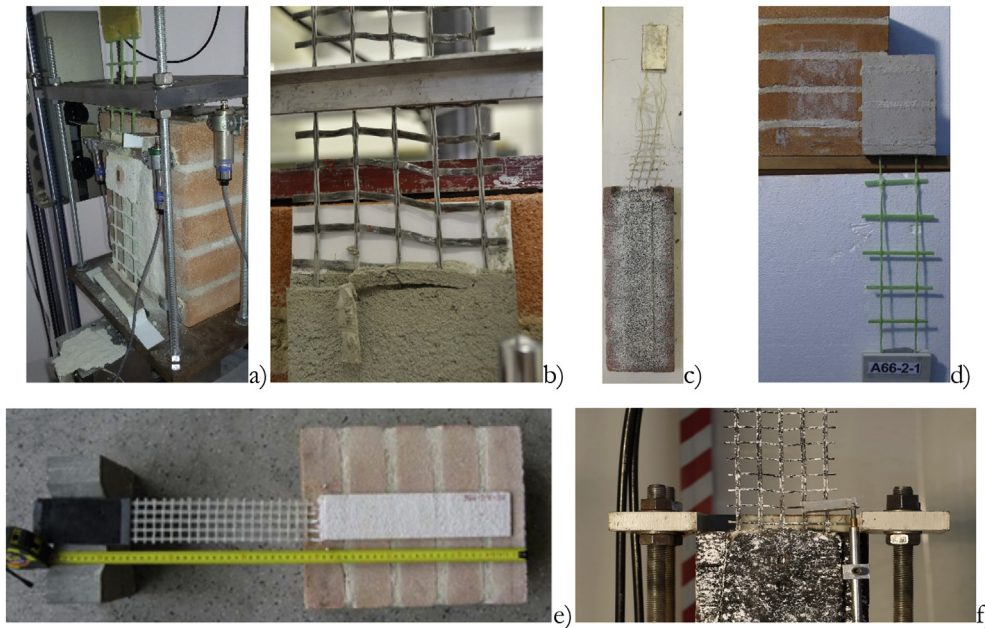
Fig. 14. Bond failure: (a) Mode C- Unisalento - #B-3; (b) Mode E + F- Polimi - #G; (c) Mode F- Unirm3 - #F; (d) Mode B- Units - #B-4; (e) Mode F- Cut - #C; (f) Mode D + F- Unina - #H.

behaviour of FRCM and FRP composites, as for the last the "Mode A" is the typical failure mode occurring when the composite is applied to the masonry substrates.

The experimental results are compared and discussed in the following. The analysis is made in terms of axial strength of the FRCM reinforcement, mode of failure and axial stress-versus slip curves (Fig. 15), when available. When at least two laboratory tested the same FRCM system, a comparison is made between obtained results; in the other cases, the results reported are anyhow considered a useful contribution to increase the existing experimental database, still limited on this topic and to get more insight on the bond behaviour of FRCM systems even never tested before. .

The tests performed at Polimi and ZAG laboratories on #A GFRCM reinforcement present similar results in terms of ultimate

load and axial strength (Table 7), despite the different test set-up utilized (double lap shear test at ZAG and single lap shear test at Polimi). In fact for the strength values the difference is approximately 5%; as expected, a larger difference was obtained in terms of slip (17%). As reported in Table 7 the specimens failed in different modes: at ZAG all samples failed due to tensile rupture of the fiberglass; the failure occurred in different locations along the length of the textile, but always outside the bonded region. On the contrary, the bond failure observed for tests at Polimi is characterized by the slippage of the textile within the matrix with or without mortar cracking. The exploitation rate (σ_f/σ_U) ranged from 35% to 45%. The comparison in terms of axial stress versus slip is reported in Fig. 15a; analysing the curves a significant difference can be observed, especially referring to the slope of the ascending

Table 7
Experimental bond test results.

FRCM type	Lab	Slip type	Load F_{max}		Slip s		$\sigma_f = F_{max}/A_f$	Failure mode	σ_f/σ_u
			[N]	COV [%]	[mm]	COV [%]	[MPa]		[%]
#A	ZAG	f-s	1196	25	0,75	22	299	F	47
	Polimi	f-s	1265	14	0,64	32	316	D-E	35
#B-1	Unisalento	m-s	4793	23	0,31	39	420	C	27
#B-2	Unipg	f-s	14737	16	4,34	20	970	C	−
	Units	m-s	16407	6	0,05	7	1079	E-C	−
#B-3	Uminho (l = 120 mm)	f-s	7446	15	0,96	59	980	F-B	−
	Uminho (l = 180 mm)	f-s	8284	11	0,75	18	1090	F	−
#B-4	Unipg (l = 120 mm)	f-s	7166	25	0,11	154	942	C-F	70
	Units (l = 240 mm)	m-s	9514	5	0,04	63	1252	F	94
#C	Unibo	f-s	2885	8	0,70	37	801	F	69
	Cut	f-s	2631	17	0,81	46	731	F	59
#D-1	Unisalento	m-s	1163	14	0,01	25	351	D	108
#D-2	Unipd	f-s	609	16	0,44	57	420	F	96
#E	Upatras	f-s	2130	7	2,17	19	570	D/F	41
	Unirm3	f-s	1500	5	2,34	13	644	F	52
	Unipd	f-s	2092	6	3,54	32	558	D/F	−
#F	Unirm3	f-s	1550	8	1,27	17	1098	F	51
	Unifi	f-s	1478	9	2,57	27	1049	F	108
	Unipd	f-s	1483	4	1,33	65	1052	F	132
	Uminho	f-s	1380	10	1,26	50	979	F	75
	Unibo	f-s	1254	9	0,95	6	889	F	71
#G	Polimi	f-s	3020	9	4,58	29	671	E/F	58
	Zag	f-s	3987	6	4,05	5	886	F	−
#H	Unina	f-s	1996	28	1,19	62	456	D/F	57
	Unisannio	m-s	2569	40	0,03	42	734	F	58
	Uminho	f-s	2700	15	1,15	25	771	D/F	113

branch. This occurrence may be related to the different utilized experimental set-up, a double face shear test at Zag and a single face shear test at Polimi, besides the different ends preparation, namely the absence of ends tabs and the use of steel tabs at ZaG and Polimi, respectively. As known the double lap configuration often involves eccentricity effects as well as gripping the bare mesh may cause uneven load distribution between glass strands, that could be the cause of the unexpected slope trend of the curves obtained at the ZAG lab. Similar considerations may be extended to the #G system discussed in the following.

Tests conducted by Unipg and Units on masonry prisms with type #B-2 GFRCMs show similar results in terms of ultimate load and axial strength; the difference between the average load values being approx. 10%. The method used to measure the slip by the two laboratories was different, fibre-substrate in the case of Unipg and mortar-substrate at Units; therefore, the comparison in terms of axial stress versus slip curve is meaningless. An inter-laminar shear mode of failure was observed at both Units and Unipg with slippage of the textile with respect to the cracked matrix and subsequent debonding of the top layer of mortar (plus textile) at the textile-to-bottom mortar layer interface. A high scatter was observed for results obtained testing type #B-4 GFRCM system that differs from the #B-2 one in grid spacing (66 mm and 33 mm for the former and the latter, respectively). The difference between the results of the two laboratories (Units and Unipg, for specimens with bond length equal to 240 mm) in terms of axial strength is about 25%. Again, the slips have been recorded with different procedures by the labs, therefore the comparison of the axial stress-slip curves is not reported. However, it is evident that the slips measured between the composite and the substrate are generally lower (by an order of magnitude) than those measured between the textile and the substrate (see also results for #D FRCMs). Regarding the mode of failure, it was similar to that observed for type #B-2 GFRCM materials at Unipg whereas the textile rupture at the bare grid was observed for specimens tested at Units; in the latter case, specimens failed under mode "F" at an axial stress level close to the

GFRCM tensile strength, as demonstrated by the high value of the ratio σ_f/σ_u (94%).

A good level of repeatability was obtained for test performed at Unibo and Cut on specimens with type #C GFRCM, as all analysed parameters exhibited low values of CoV (about 10%). In addition, the axial stress versus slip curves (Fig. 15b) are very similar and all specimens failed by textile rupture at the unbonded region (Fig. 14f); the formation of longitudinal and transverse cracks on the reinforcement was recorded at Cut Lab. The exploitation ratio for this material ranged from 60 to 70%.

Specimens with type #D GFRCM bonded strip were tested at Unisalento and Unipd; different yarns' spacing (15 mm at Unisalento and 7,6 mm at Unipd) were employed. It is therefore possible to compare the data in terms of axial stress. The average maximum axial stress obtained by the two laboratories is similar; the difference being approximately equal to 16%. The different methods used to measure slip values between labs did not allow the comparison of the axial stress versus slip curves. The modes of failure observed were also different: slippage of the textile within the matrix at Unisalento and rupture of the textile at the bonded region at Unipd. However, the values of σ_f/σ_u suggest that – in both cases – the tensile strength of the FRCM material was attained.

The average value of the axial strength obtained for type #E system is equal to 591 MPa (COV = 8%). By comparing the axial stress vs slip curves (Fig. 15c), it is possible to note that the slope of the first part of the curves is fairly comparable for all cases while the trend of the post peak curves is significantly different for Unipd. The bond failure occurred due to the tensile rupture of the textile outside the bonded area with or without slippage of the fibre at the mortar-fibre interface. The exploitation ratio is 40–50%.

The tests performed at Unirm3, Unifi, Unipd, Uminho and Unibo on type #F reinforcing system show a mode "F" of failure (Fig. 14e) without mortar cracks. The ultimate loads as well as the axial strength are similar with an average value of $\sigma_f = 1013,4$ MPa (COV = 8%). The experimental axial stress versus slip curves are plotted in Fig. 15d. In the graph the results obtained at Uminho are
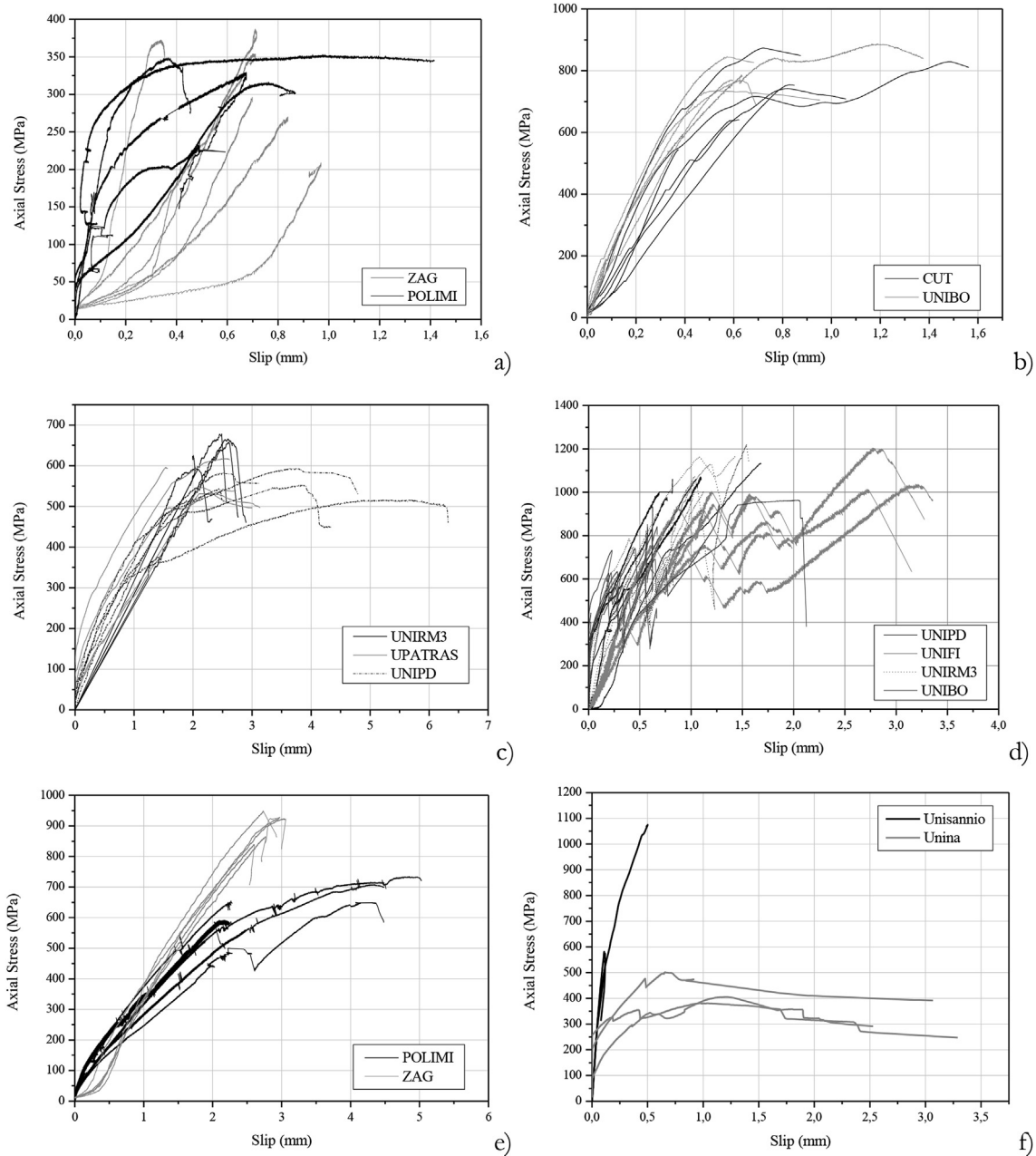
Fig. 15. Axial stress versus slip curves: (a) #A; (b) #C; (c)#E; (d)#F; (e) #G; (f)#H.

disregarded as the slip measurement was affected by the progressive fibres failure. Overlap of curves hinders a clear comparison between them. However, they are characterized by multiple load drops due to the progressive fibres rupture and the consequent redistribution of the load between the remaining fibres. The σ_f/σ_u values are high except in the case of Unirm3 that, nevertheless, registered the highest value of the tensile strength (Table 5).

Different results were obtained at Polimi and ZAG from the tests on type #G reinforcement. The ultimate load and the axial strength differ by approximately 25% (Table 7), while the scatter is lower in terms of slip (13%). The significant difference between the slope of the first branch of the axial stress-slip curves (Fig. 15e) can be explained as for the case of type #A specimens, reported above. The modes of failure "E" and "F" were observed at Polimi; the tensile rupture of the fibre at the loaded end of the bonded area was

observed at ZAG.

Finally, by comparing the test results on type #H system, it is possible to note that similar stress values were obtained at Uminho and Unisannio, while lower average values (25%) have been recorded at Unina, (Table 7). Moreover, it is worth noting that for the tests of Unina and Unisannio the ratio σ_t/σ_u was 56–57%, while for the tests of Uminho it resulted about double (113%). This was partially due to the fact that the average value of σ_u obtained by Uminho was lower than the values recorded in the other two laboratories (i.e., 680 MPa vs 800 and 900 MPa); such difference between the results was further due to the high sensitivity of grid type #H to possible misalignment of the rovings because of the large mesh spacing. Different set-ups may be, indeed, responsible of different accuracy in the alignment of all the rovings with respect to the loading direction. This is, for example, confirmed by the results

of Unisannio since, although the failure mode was always due to the tensile failure of the fibres, it occurred at very variable load levels (i.e. CoV = 40%). The comparison in terms of axial stress-slip curves between the data obtained at Unina and Unisannio is reported in Fig. 15f; the data show high scatter in terms of both the shape of the curves and the maximum tensile stresses, as already mentioned. In particular, the different shape of the curves and the lower values of slips recorded at Unisannio are probably due to the different measurement methods used in the two laboratories (strain gauges at Unisannio and displacement transducers at Unina).

3.7. Bond test results: experimental comparison

On the basis of the results reported in the previous section, it seems reasonable to classify the GFRCM materials tested in three types: (1) GFRCM made of dry glass fibre, lime mortar and bond enhancing agents (Fig. 16a); (2) reinforcements made of dry glass fibre and lime mortar (Fig. 16b); (3) reinforcements made of GFRP and cement or lime-based mortars (Fig. 16c). Each comparison reports the experimental points, the mean value (dashed line) and the standard deviation (hatched area). Fig. 16a and c show that, in general, test results are comparable. In particular, for #B-2/3/4 materials it is possible to observe that the grid spacing and the mechanical proprieties of the mortar did not affect the axial strength, that results is in average equal to σ_f = 1093 MPa (CoV = 12%). An average value can be also calculated for GFRCM materials with a bond enhancing agent: σ_f = 659 MPa (COV = 21%). On the contrary, the dispersion of the data increased when looking at the reinforcement made by dry glass fibres and lime mortar (Fig. 16b); in this case, results in terms of axial strength

(σ_f = 717 MPa) presented a high value of the coefficient of variation, CoV = 50%. As a consequence, even if the bond performances of the last two categories are similar in terms of mean values, when dealing with characteristic values, generally utilized for design purposes, the last system could be strongly penalized. Most likely, the stress transfer mechanism is different for the categories considered depending on the type of mortar, its physical and mechanical properties, and on the kind of the grid. In particular, the experimental program carried out shows that the weakest interface is generally that between mortar and reinforcement; however, in some cases the chemical bond contribution is prevailing (case of dry fibers), and it may be greatly improved by the presence of bond enhancing agents; in other cases, a mechanical bond contribution should be also considered (pre-impregnated grid). Future research work should be addressed to the evaluation of the effects of the mentioned parameters on the bond performance in order to furnish useful design provisions, as well as to the optimization of the testing procedure.

4. Conclusions

In this paper, a Round Robin experimental activity on the tensile and bond behaviour of GFRCM specimens is reported and discussed. Fifteen European laboratories were involved in the study of eight different GFRCM materials. In total, 255 specimens have been tested.

Test results were analysed and compared in order to enrich the existing knowledge on GFRCM materials and focus on their mechanical behaviour. The great variability of the systems analysed in terms of the constituent materials has caused a great dispersion of
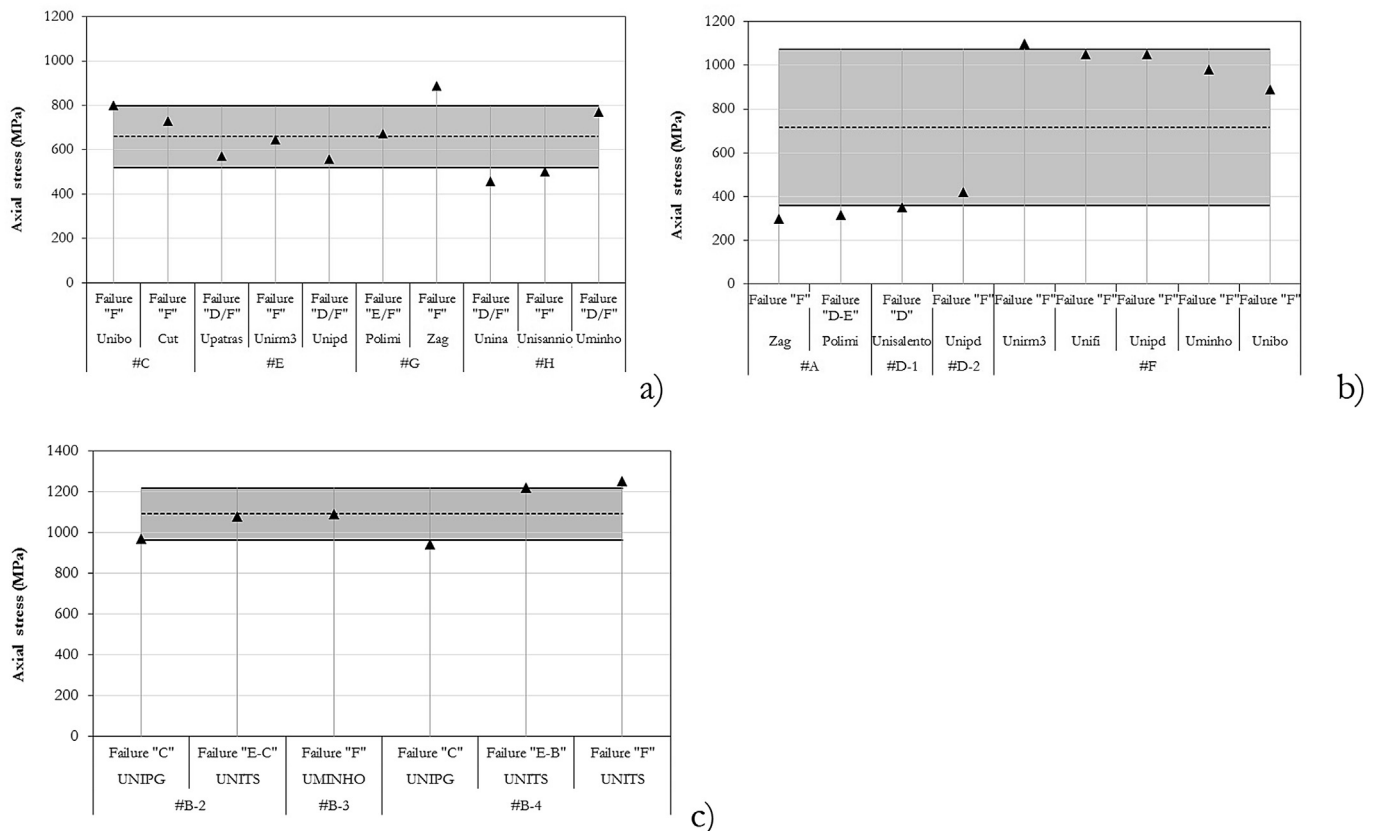
Fig. 16. Comparison of axial strength: (a) GFRCM AR textile with coating + lime-based mortar; (b) GFRCM without coating + lime based mortar; (c)GFRCM with Resin-impregnated AR textile + lime or cement-based mortar.

the experimental results, often difficult to treat. However, the authors, starting with the lack of technical documentation on the subject and the increase of interest for these strengthening systems believes that the round robin results could be very useful to the scientific community to enlarge the knowledge in the treated field.

The stress-strain curves obtained from tensile tests are mainly characterized by two phases. In the first stage, the behaviour is governed by both the mortar and the glass fibre textile. Once the first mortar cracking occurs, the specimen axial stiffness decreases and the tension stiffening contribution due to the mortar between cracks plays a relevant role. By further increasing the load, the cracking evolves until the tensile behaviour remains only governed by the fibres. However, it is worth noting that not all the reinforcement systems tested are able to exploit the same tension stiffening effect that depends on mortar properties, geometrical layout of the grid (spacing between rovings) interface properties (presence of coating, etc.). A large scatter was generally observed in terms of axial strain, probably a larger gauge length could be able to furnish a better accuracy and reliability of results. Moreover, it was noted that higher scatter between experimental test were recorded when the clamping system was different. An in depth analysis could help to better understand how the system used to apply the load influences the experimental results; therefore a specific research work is suggested to investigate the influence of this parameter.

Different failure modes were detected; the most common type is the mortar cracking and tensile failure of glass fibre; in many cases, also slippage of the textile at clamps was reported. This failure is probably related to the specific gripping system involved and to the lateral pressure applied by the machine grips.

Finally, based on the obtained results it appears evident the necessity of a preliminary knowledge of the constituent materials (i.e. fibre grid and mortar) as well as of their interface in order to better understand the mechanical behaviour of the GFRCM.

By analysing the results on bond between GFRCM and masonry, it is possible to summarize the following points.

- The test results showed a good level of repeatability in terms of axial strength and modes of failure when referring to the same composite. The data furnished a high level of scatter when two different test set-up were compared, i.e. double and single lap shear test. This results further underlines the need of defining a standard procedure for studying the bond behaviour between GFRCM and masonry substrate; -Analyses and comparisons were mainly made in terms of axial strength. However, in the future it should be important to define a bond stress, related to the kind of interface mainly involved in the bond transfer mechanism. In particular, it could be important to classify the bond results according to the mode of failure and to define the most appropriate parameters, able to describe and discuss the interfacial behaviour.
- Similarly to the tensile tests, several modes of bond failure were detected by the bond test under shear load. However, a cohesive failure of the reinforcement from the substrate never occurred. It is enough clear that the stress transfer mechanism between GFRCM and substrate is different from that experienced for FRP materials: the GFRCM are not able to achieve the maximum cohesive bond failure because the failure of the fibres occurs first.
- A refinement of the bond test procedure is needed referring to the kind of measures to be made and also to the possibility of considering different testing procedure in relation to the reinforcing system. Results in terms of slip values are more scattered but the complexity of the measurement of this parameter is well known. Thus, it emerged the need of recording different slip measurements (i.e. fibres-substrate or mortar-substrate). In

particular, future investigations should be carried out by measuring the slips between fibre and mortar, between mortar and substrate and between fibres and substrate. In fact, when dry glass fibre are used the measuring of the slip could refers to the relative displacement between fibre and matrix, on the contrary for the system with FRP fibre the measure could refer to the slip fibre-substrate.

- Finally, the high dispersion of the test results makes difficult to perform all necessary comparisons and to calibrate design formulas. However, the data obtained represent an important contribution to the understanding of the general physical phenomena that characterise the mechanical behaviour of GFRCM materials and their bond with masonry structures. Starting from obtained results the future research activity may be focused on critical or lacking aspects here evidenced, finally aiming to draw design provisions, needed to further promote the diffusion of this successful strengthening technique. That success is mostly linked to the low cost of the glass fibres with respect to other kinds of fibres (i.e. carbon), especially for application on the vernacular historic building where the use of high performing material is often unnecessary.

References

[1] Eshani MR, Saadatmanesh H. Shear behaviour of URM retrofitted with FRP overlays. J Compos Constr 1997;1(1):17—25.
[2] Avvakumovits O. Seismic evaluation and retrofitting of existing unreinforced masonry buildings. Proc 13th Struct Congr 1995:1821—4. Boston MA.
[3] Triantafillou TC. Strengthening of masonry laminates using epoxi-bonded FRP laminates. J Compos Constr 1998;2(2):96—104.
[4] Valluzzi MR, Tinazzi D, Modena C. Shear behaviour of masonry panels strengthened by FRP laminates. Constr Build Mater 2002;16:409—16.
[5] Stratford T, Pascale G, Manfroni O, Bonfiglioli B. Shear strengthening masonry panels with sheet glass-fibre reinforced polymer. J Compos Constr 2004;8(5): 434—43.
[6] Roca P, Araiza G. Shear response of brick masonry small assemblages strengthened with bonded FRP laminates for in-plane reinforcement. Constr Build Mater 2010;24:1372—84.
[7] Costa AA, Arede A, Costa A, Oliveira CS. In situ cyclic tests on existing stone masonry walls and strengthening solutions. Earthq Eng Struct Dynam 2011;40:449—71.
[8] Malena M, Focacci F, Carloni C, de Felice G. The effect of the shape of the cohesive material law on the stress transfer at the FRP-masonry interface. Compos Part B Eng 2017;110(1):368—80.
[9] Alotaibi KS, Galal K. Axial compressive behavior of grouted concrete block masonry columns confined by CFRP jackets. Compos Part B Eng 2017;114(1 April):467—79.
[10] Valluzzi MR, Valdemarca M, Modena C. Behaviour of brick masonry vaults strengthened by FRP laminates. J Compos Constr 2001;5(3):163—9.
[11] Foraboschi P. Strengthening of masonry arches with fibre-reinforced polymer strips. J Compos Constr 2004;8(3):96—104.

[12] Briccoli Bati S, Rovero L, Tonietti U. Strengthening masonry arches with composite materials. J Compos Constr 2007;11(1):33—41.

[13] Oliveira D, Basilio I, Lourenço P. Experimental behaviour of FRP strengthened masonry arches. J Compos Constr 2010;14(3):312—22.

[14] Caporale A, Feo L, Luciano R, Penna R. Numerical collapse load of multi-span masonry arch structures with FRP reinforcement. Compos B Eng 2013;54(1): 71—84.

[15] Caporale A, Feo L, Hui D, Luciano R. Debonding of FRP in multi-span masonry arch structures via limit analysis. Compos Struct 2014;108(1):856—65.

[16] Corradi M, Borri A, Castori G, Coventry K. Experimental analysis of dynamic effects of FRP reinforced masonry vaults. Materials 2015;8:8059—71.

[17] Krevaikas TD, Triantafillou TC. Masonry confinement with fibre-reinforced polymers. J Compos Constr 2005;9(2):128—35.

[18] Aiello MA, Micelli F, Valente L. Structural upgrading of masonry columns by using composite reinforcements. J Compos Constr 2007;11(6):650—8.

[19] Aiello MA, Micelli F, Valente L. FRP confinement of square masonry columns. J Compos Constr 2009;13(2):148—58.

[20] Di Ludovico M, D'Ambra C, Prota A, Manfredi G. FRP confinement of tuff and clay brick columns: experimental study and assessment of analytical models. J Compos Constr 2010;14(5):583—96.

[21] C Martinelli E, Paciello S, Camorani G, Aiello MA, Micelli F, Nigro E. Masonry columns confined by composite materials: experimental investigation. Compos B Eng 2011;42(4):692—704.

[22] Prota A, Marcari G, Fabbrocino G, Manfredi G, Aldea C. Experimental in-plane behaviour of tuff masonry strengthened with cementitious matrix—grid composites. J Compos Constr ASCE 2006;10(3):223—33.

[23] De Santis S, de Felice G. Steel reinforced grout systems for the strengthening of masonry structures. Compos Struct 2015;134:533—48. http://dx.doi.org/10.1016/j.compstruct.2015.08.094.

[24] Lignola GP, Angiuli R, Prota A, Aiello MA. FRP confinement of masonry: analytical modeling. Mater Struct 2014;47(12):2101—15.

[25] Minafò G, D'Anna J, Cucchiara C, Monaco A, La Mendola L. Analytical stress-strain law of FRP confined masonry in compression: literature review and design provisions. Compos Part B Eng 2017;115:160—9. 15 April.

[26] Valluzzi MR, Oliveira D, Caratelli A, Castori G, Corradi M, De Felice G, et al. Round robin test for composite-to-brick shear bond characterization. Mater Struct 2012;45:1761—91.

[27] Carozzi FG, Poggi C. Mechanical properties and debonding strength of Fabric Reinforced Cementitious Matrix (FRCM) systems for masonry strengthening. Compos Part B 2015;70:215—30.

[28] De Santis S, de Felice G. Tensile behaviour of mortar-based composites for externally bonded reinforcement systems. Compos Part B-Eng 2015;68: 401—13. http://dx.doi.org/10.1016/j.compositesb.2014.09.011.

[29] De Felice G, Aiello MA, Bellini A, Ceroni F, De Santis S, Garbin E, et al. Experimental characterization of composite-to-brick masonry shear bond. Mater Struct 2015:1—16.

[30] Mazzotti C, Ferracuti B, Bellini A. Experimental bond tests on masonry panels strengthened by FRP. Compos Part B Eng 2015;80:223—37.

[31] Mazzotti C, Murgo FS. Numerical and experimental study of GFRP-masonry interface behaviour: bond evolution and role of the mortar layers. Compos Part B Eng 2015;75:212—25.

[32] Kwiecien A, de Felice G, Oliveira DV, Zając B, Bellini A, De Santis S, et al. Repair of composite-to-masonry bond using flexible matrix. Mater Struct 2016;49(7):2563—80.

[33] Garbin E, Panizza M, Valluzzi MR. Experimental assessment of bond behaviour of FRP on brick masonry. IABSE Struct Eng Int 2010;20(4):392—9.

[34] Carloni C, Subramaniam KV. FRP-masonry debonding: numerical and experimental study of the role of mortar joints. ASCE J Compos Constr 2012;16(5): 581—9.

[35] Carloni C, Focacci F. FRP-masonry interfacial debonding: an energy balance approach to determine the influence of the mortar joints. Eur J Mech A/Solids 2016;55:122—33.

[36] Leone M, Stijn M, Aiello MA. Effect of elevated service temperature on bond between FRP EBR system and concrete. Compos Part B 2009;40:85—93.

[37] Aiello MA, Leone M. Interface analysis between FRP EBR system and concrete. Compos Part B Eng 2008;39B(No.4):618—26. Elsevier.

[38] Hadigheh SA, Gravina RJ. Generalization of the interface law for different FRP processing techniques in FRP-to-concrete bonded interfaces. Compos Part B Eng 2016;91(15):399—407. April 2016.

[39] Carloni C, Subramaniam KV. FRP-masonry debonding: numerical and experimental study of the role of mortar joints. ASCE J Compos Constr 2012;16(5): 581—9.

[40] Maljaee H, Ghiassi B, Lourenço PB, Oliveira DV. Moisture-induced degradation of interfacial bond in FRP-strengthened masonry. Compos Part B Eng 2016;87(15):47—58. February.

[41] ACI 440.7R-10. Guide for design and construction of externally bonded FRP systems for strengthening unreinforced masonry structures. 2010. ACI Committee 440, Farmington Hills.

[42] CNR DT200/R1. Guide for the design and construction of an externally bonded FRP system for strengthening existing structures. Rome: Italian National Research Council; 2013.

[43] Aiello MA, Sciolti MS. Bond analysis of masonry structures strengthened with CFRP sheets. Constr Build Mater 2006;20(1):90—100.

[44] Briccoli Bati S, Rotunno T. GFRCM and CFRP composite materials in masonry reinforcement. In: Proceedings ninth international conference on composites

[45] S. Briccoli Bati, I. Feletti, T. Rotunno, "Reinforcement with GFRCM of structural masonry elements: experimental studies of in scale models", Proceedings of the International Conference Composites in Constructions, Cosenza, Italy, September 16-19 2003, pagg. 165-170, ISBN: 88-7740-358-6Crossref Partial Au1 Au2 Au3 ATL STL Year.

[46] Ascione L, de Felice G, De Santis S. A qualification method for externally bonded Fibre Reinforced Cementitious Matrix (FRCM) strengthening systems. Compos Part B-Eng 2015;78:497—506. http://dx.doi.org/10.1016/j.compositesb.2015.03.079.

[47] Papanicolaou CG, Triantafillou TC, Karlos K, Papathanasiou M. Textile-reinforced mortar (TRM) versus FRP as strengthening material of URM walls: in-plane cyclic loading. Mater Struct 2007;40(10):1081—97.

[48] Papanicolaou CG, Triantafillou TC, Papathanasiou M, Karlos K. Textile-reinforced mortar (TRM) versus FRP as strengthening material of URM walls: out-of-plane cyclic loading. Mater Struct 2008;41(1):143—57.

[49] Garmendia L, San-José JT, García D, Larrinaga P. Rehabilitation of masonry arches with compatible advanced composite material. Constr Build Mater 2011;25(12):4374—85.

[50] Corradi M, Borri A, Castori G, Sisti R. Shear strengthening of wall panels through jacketing with cement mortar reinforced by GFRP grids. Compos B Eng 2014;64:33—42.

[51] Borri A, Castori G, Corradi M, Sisti R. Masonry wall panels with GFRP and steel-cord strengthening subjected to cyclic shear: an experimental study. Constr Build Mater 2014;56:63—73.

[52] Gattesco N, Boem I. Experimental and analytical study to evaluate the effectiveness of an in-plane reinforcement for masonry walls using GFRP meshes. Constr Build Mater 2015;88:94—104.

[53] Gattesco N, Boem I, Dudine A. Diagonal compression tests on masonry walls strengthened with a GFRP mesh reinforced mortar coating. Bull Earthq Eng 2015;13(6):1703—26.

[54] Borri A, Corradi M, Sisti R, Buratti C, Belloni E, Moretti E. Masonry wall panels retrofitted with thermal-insulating GFRP-reinforced jacketing. Mater Struct 2015:1—12.

[55] Gattesco N, Amadio C, Bedon C. Experimental and numerical study on the shear behaviour of stone masonry walls strengthened with GFRP reinforced mortar coating and steel-cord reinforced repointing. Eng Struct 2015;90: 143—57.

[56] Borri A, Castori G, Corradi M. Behaviour of thin masonry arches repaired using composite materials. Compos B Eng 2015;87:311—21.

[57] Kim HY, Park YH, You YJ, Moon CK. Durability of GFRP composite exposed to various environmental conditions. KSCE J Civ Eng 2006;10(4):291—5.

[58] Willis CR, Yang Q, Seracino R, Griffith MC. Bond behaviour of FRP-to-clay brick masonry joints. Eng Struct 2009;31:2580—7.

[59] Righetti L, Corradi M, Borri A, Castori G, Sisti R, Osofero AI. Durability of GFRP grids for masonry structures. Int J Forensic Eng 2016;3(1—2):164—79.

[60] Carloni C, D'Antino T, Sneed LH, Pellegrino C. Role of the matrix layers in the stress-transfer mechanism of FRCM composites bonded to a concrete substrate. ASCE J Eng Mech 2015;141(6):10. 1061/(ASCE)EM.1943-7889.0000883.

[61] Ombres L. Analysis of the bond between fabric reinforced cementitious mortar (FRCM) strengthening systems and concrete. Compos Part B 2015;69: 418—26.

[62] Tetta ZC, Koutas LN, Bournas DA. Textile-reinforced mortar (TRM) versus fiber-reinforced polymers (FRP) in shear strengthening of concrete beams. Compos Part B 2015;77(2015):338—48.

[63] De Santis S, Carozzi FG, de Felice G, Poggi C. Test methods for Textile Reinforced Mortar systems. Compos Part B-Eng http://dx.doi.org/10.1016/j.compositesb.2017.03.016.

[64] Carozzi FG, Bellini A., D'Antino T., de Felice G., Focacci F., Hojdys L., Laghi L., Lanoye E., Micelli F., Panizza M., Poggi C., Experimental investigation of tensile and bond properties of Carbon-FRCM composites for strengthening masonry elements. Compos Part B http://dx.doi.org/10.1016/j.compositesb.2017.06.018.

[65] Lignola G.P., Caggegi C, Ceroni F., De Santis S., Krajewski P., Lourenço P.B., Morganti M., Papanicolaou C.G., Pellegrino C., Prota A., Zuccarino L. Performance assessment of basalt FRCM for retrofit applications on masonry. Compos Part B-Eng http://dx.doi.org/10.1016/j.compositesb.2017.05.003.

[66] Caggegi C., Carozzi F.G., De Santis S., Fabbrocino F., Focacci F., Hojdys L., Lanoye E., Zuccarino L. Experimental analysis on tensile and bond properties of PBO and Aramid fabric reinforced cementitious matrix for strengthening masonry structures. Compos Part B-Eng http://dx.doi.org/10.1016/j.compositesb.2017.05.048.

[67] Sneed LH, D'Antino T, Carloni C, Pellegrino C. A comparison of the bond behaviour of PBO-FRCM composites determined by single-lap and double-lap shear tests. Cem Concr Compos 2015;64:37—48.

[68] De Santis S., Ceroni F., de Felice G., Fagone M., Ghiassi B., Kwiecień A., Lignola G.P., Morganti M., Santandrea M., Valluzzi M.R., Viskovic A., Round Robin Test on tensile and bond behaviour of Steel Reinforced Grout systems. Compos Part B-Eng http://dx.doi.org/10.1016/j.compositesb.2017.03.052.

[69] Brameshuber W. RILEM TC 232-TDT: recommendation of RILEM TC 232-TDT: test methods and design of textile reinforced concrete. Uniaxial tensile test: test method to determine the load bearing behaviour of tensile specimens made of textile reinforced concrete. In: Materials and structures RILEM, vol 49; 2016. Nr. 5.

[70] UNI EN 998—2. Specification for mortar for masonry - masonry mortar. 2010.